Robust Sidelobe Control via Complex-Coefficient Weight Vector Orthogonal Decomposition

Xuejing Zhang, *Student Member, IEEE*, Zishu He, *Member, IEEE*, Xuepan Zhang, and Julan Xie

***Abstract*— This paper presents a new array response control algorithm named complex-coefficient weight vector orthogonal decomposition (C^2-WORD), and its application to robust sidelobe control and synthesis in the presence of steering vector mismatch. The proposed C^2-WORD algorithm is a modified version of the existing WORD approach. We extend WORD by allowing a complex-valued combining coefficient in C^2-WORD, and then determine the optimal combining coefficient by maximizing the white noise gain. Moreover, assuming that the steering vector uncertainty is norm-bounded, we further devise a robust C^2-WORD algorithm, which is able to precisely control the upper boundary response level of a sidelobe point as desired. To enhance the practicality of the proposed robust C^2-WORD algorithm, we also study how to determine the upper norm boundary of steering vector uncertainty under various mismatch circumstances. By applying the robust C^2-WORD algorithm iteratively, a robust sidelobe synthesis approach is developed. Contrary to the existing approaches, the devised robust C^2-WORD algorithm offers an analytical expression of weight vector updating and can work starting from an arbitrarily specified weight. Simulation results are presented to validate the effectiveness and good performance of the robust C^2-WORD algorithm on sidelobe control and synthesis in the presence of steering vector uncertainties.**

***Index Terms*— Array pattern synthesis, robust sidelobe control, robust sidelobe synthesis, steering vector mismatch.**

I. Introduction

ARRAY antenna has found numerous applications to radar, navigation, and wireless communication. Determining the complex weights for array elements to achieve the desired beampattern is a fundamental problem [1]–[3]. Quite a number of approaches to array response control or pattern synthesis have been reported during the past several decades [4]–[7]. In most existing work, the array steering vectors are assumed to be known exactly. Under practical circumstances, however, the actual steering vectors may be different from the assumed (or ideal) ones. The steering vector uncertainty can be caused by various factors, such as, channel gain-phase mismatch, element position mismatch, and mutual coupling effect. The existence of steering vector uncertainties may lead to performance degradation for the existing array response control or pattern synthesis approaches.

During the past several decades, quite a number of robust algorithms have been developed to control array response or synthesize desirable beampatterns with steering vector uncertainties. For example, Yan and Hovem [8] proposed a powerful robust approach to synthesizing array patterns with low sidelobes in the presence of unknown array manifold perturbations. This approach optimizes the worst-case performance of sidelobe response by formulating the robust pattern synthesis problem as a convex programming (CP) form. Nevertheless, this method can only synthesize uniform sidelobes and may not work well if the desired sidelobe shape is nonuniform. A novel robust beampattern synthesis method is proposed in [9], where the mutual coupling effect is considered and two optimization methods are provided. Nevertheless, the mutual coupling matrix has to be precalculated in this approach before the synthesis process. Efficient robust broadband antenna array pattern synthesis techniques in the presence of array imperfections have been presented in [10], where nine different optimization criteria are provided with each one having particular advantage and disadvantage for certain applications. In contrast to the above deterministic pattern synthesis methods, there are also some excellent works considering robust adaptive beamforming in the presence of steering vector uncertainties (see [11]–[15]). In this scenario, it is usually required to shape satisfactory beampatterns and reject the undesirable interferences. In addition, it should be pointed out that our discussion is different from the pattern tolerance analyses studied in [16]–[20], where the weight vector (but not the steering vector) suffers from perturbation.

In general, the existing methods cannot flexibly control the array response starting from an arbitrarily specified weight vector. As a result, the weight vector has to be completely redesigned even if only a slight change of the desired pattern is needed. This motivates us to develop a new array response control algorithm in the presence of steering vector perturbations. Toward this end, in this paper, we first develop a scheme named complex-coefficient weight vector orthogonal decomposition (C^2-WORD), by allowing a complex-valued combining coefficient in the existing WORD algorithm in [21]. The C^2-WORD algorithm has an analytical

Manuscript received July 19, 2018; revised January 15, 2019; accepted April 27, 2019. Date of publication May 20, 2019; date of current version August 12, 2019. This work was supported in part by the National Nature Science Foundation of China under Grant 61671139, Grant 61671137, Grant 61701499, and Grant 61871085, in part by the Fundamental Research Funds for the Central Universities under Grant 2672018ZYGX2018J010, and in part by China Scholarship Council. *(Corresponding author: Xuejing Zhang.)*

X. Zhang, Z. He, and J. Xie are with the School of Information and Communication Engineering, University of Electronic Science and Technology of China, Chengdu 611731, China (e-mail: xjzhang7@163.com; zshe@uestc.edu.cn; julanxie@uestc.edu.cn).

X. Zhang is with the Qian Xuesen Laboratory of Space Technology, Beijing 100094, China (e-mail: zhangxuepan@qxslab.cn).

This paper has supplementary downloadable material available at http://ieeexplore.ieee.org, provided by the author. This file contains the MATLAB codes for reproducing partial results in this work, which is made available for personal purpose. This article is 64 KB in size.

Color versions of one or more of the figures in this paper are available online at http://ieeexplore.ieee.org.

Digital Object Identifier 10.1109/TAP.2019.2916640

solution and performs better than WORD in the sense of white noise gain (WNG) [22]–[24]. On this basis, we devise a robust C^2-WORD algorithm. Starting from any given weight vector, the proposed robust C^2-WORD algorithm can control the array response level of a single sidelobe point when array suffers from unknown steering vector mismatches. More specifically, assuming that the steering vector perturbation is norm-bounded by a known constant, we analyze the worst-case (upper and lower) boundaries of array response level. Then, given a sidelobe angle to be controlled, its desired upper response level, and an arbitrarily specified weight vector, we follow the model of C^2-WORD and propose to accurately control the worst-case upper boundary response level as desired. As presented later, the robust C^2-WORD algorithm offers an analytical expression of weight vector updating and results in small worst-case perturbation on the array response. In addition, inheriting the advantages of C^2-WORD, our robust C^2-WORD approach results in small pattern variations on the uncontrolled points. To enhance the practicality of the devised algorithm, we also give a presention on how to determine the norm boundary of steering vector uncertainty, in the cases where array suffers from channel gain-phase mismatch, element position mismatch, and mutual coupling effect. By applying the robust C^2-WORD algorithm successively, we devise an effective robust sidelobe synthesis method. Simulations show that our algorithm works well under various circumstances.

This paper is organized as follows. The proposed robust C^2-WORD algorithm is presented in Section II. In Section III, some practical considerations are provided to improve the practicality of the robust C^2-WORD algorithm. The application of robust C^2-WORD to robust sidelobe synthesis is discussed in Section IV. Representative simulations are carried out in Section V and the conclusions are drawn in Section VI.

Notations: We use bold upper case and lower case letters to represent matrices and vectors, respectively. In particular, we use $\mathbf{I}$ to denote the identity matrix. $j \triangleq \sqrt{-1}$. $(\cdot)^{\mathrm{T}}$ and $(\cdot)^{\mathrm{H}}$ stand for the transpose and Hermitian transpose, respectively. $|\cdot|$ denotes the absolute value and $\|\cdot\|_2$ denotes the l_2 norm. We use $\mathbf{B}(i,l)$ for the element at the ith row and lth column of matrix $\mathbf{B}$. $\Re(\cdot)$ and $\Im(\cdot)$ denote the real and imaginary parts, respectively. $\det(\cdot)$ is the determinant of a matrix. $\propto$ means direct proportion. $\mathbb{R}$ and $\mathbb{C}$ denote the sets of all real and complex numbers, respectively. $\mathcal{R}(\cdot)$ returns the column space of the input matrix, and $\mathcal{R}^{\perp}(\cdot)$ is the orthogonal complementary space of $\mathcal{R}(\cdot)$. $\mathbf{P}_{\mathbf{Z}}$ and $\mathbf{P}_{\mathbf{Z}}^{\perp}$ represent the projection matrices onto $\mathcal{R}(\mathbf{Z})$ and $\mathcal{R}^{\perp}(\mathbf{Z})$, respectively. $\angle(\cdot)$ returns the argument of a complex number. $\mathrm{Diag}(\cdot)$ represents the diagonal matrix with the components of the input vector as the diagonal elements. Finally, $\lambda_{\max}(\cdot)$ returns the largest eigenvalue of the input matrix.

II. Robust Sidelobe Control via C^2-WORD

In order to present the proposed robust sidelobe control algorithm, we first introduce the WORD algorithm in [21] and develop the concept of C^2-WORD algorithm.

A. WORD and C^2-WORD

To begin with, we first define the array power response as $L(\theta,\theta_0) \triangleq |\mathbf{w}^{\mathrm{H}}\mathbf{a}(\theta)|^2/|\mathbf{w}^{\mathrm{H}}\mathbf{a}(\theta_0)|^2$, where $\mathbf{w}$ is the weight vector, θ_0 is the main beam axis, $\mathbf{a}(\theta)$ stands for the nominal steering vector in direction θ. The weight vector orthogonal decomposition (WORD) algorithm in [21] is able to flexibly and precisely control the array power response level at a prescribed angle on the basis of a given weight vector. More specifically, for a given weight vector $\mathbf{w}_{k-1}$, an angle θ_k to be controlled and its desired (normalized) power response level ρ_k, WORD algorithm realizes the array response control task $L_k(\theta_k,\theta_0)=\rho_k$, by updating its weight vector as

$$\mathbf{w}_k = [\mathbf{w}_{k-1,\perp} \quad \mathbf{w}_{k-1,\parallel}][1 \quad \beta_k]^{\mathrm{T}}, \quad \beta_k \in \mathbb{R} \tag{1}$$

where $L_k(\theta,\theta_0)$ represents the array power response of the weight vector $\mathbf{w}_k$, $\mathbf{w}_{k-1,\perp}$ and $\mathbf{w}_{k-1,\parallel}$ are defined as

$$\mathbf{w}_{k-1,\perp} \triangleq \mathbf{P}^{\perp}_{[\mathbf{a}(\theta_k)]}\mathbf{w}_{k-1}, \quad \mathbf{w}_{k-1,\parallel} \triangleq \mathbf{P}_{[\mathbf{a}(\theta_k)]}\mathbf{w}_{k-1} \tag{2}$$

with k denoting the step index. In (1), the real-valued β_k can be selected to be either β_a or β_b, both of which can be determined by the desired level ρ_k at θ_k. In [21], it has been derived that

$$\beta_a = \frac{-\Re(\mathbf{B}_k(1,2))+d}{\mathbf{B}_k(2,2)}, \quad \beta_b = \frac{-\Re(\mathbf{B}_k(1,2))-d}{\mathbf{B}_k(2,2)} \tag{3}$$

where $\mathbf{B}_k$ and d satisfy

$$\mathbf{B}_k = \begin{bmatrix}\mathbf{w}_{\perp}^{\mathrm{H}}\mathbf{a}(\theta_k)\\ \mathbf{w}_{\parallel}^{\mathrm{H}}\mathbf{a}(\theta_k)\end{bmatrix}\begin{bmatrix}\mathbf{w}_{\perp}^{\mathrm{H}}\mathbf{a}(\theta_k)\\ \mathbf{w}_{\parallel}^{\mathrm{H}}\mathbf{a}(\theta_k)\end{bmatrix}^{\mathrm{H}} - \rho_k\begin{bmatrix}\mathbf{w}_{\perp}^{\mathrm{H}}\mathbf{a}(\theta_0)\\ \mathbf{w}_{\parallel}^{\mathrm{H}}\mathbf{a}(\theta_0)\end{bmatrix}\begin{bmatrix}\mathbf{w}_{\perp}^{\mathrm{H}}\mathbf{a}(\theta_0)\\ \mathbf{w}_{\parallel}^{\mathrm{H}}\mathbf{a}(\theta_0)\end{bmatrix}^{\mathrm{H}} \tag{4}$$

$$d = \sqrt{\Re^2(\mathbf{B}_k(1,2)) - \mathbf{B}_k(1,1)\mathbf{B}_k(2,2)}. \tag{5}$$

In (4), $\mathbf{w}_{\perp}$ and $\mathbf{w}_{\parallel}$ are the short notations of $\mathbf{w}_{k-1,\perp}$ and $\mathbf{w}_{k-1,\parallel}$, respectively. To obtain the ultimate expression of $\mathbf{w}_k$ that adjusts the response level of θ_k to ρ_k, the one (either β_a or β_b) that minimizes $F(\beta) = \|\mathbf{P}^{\perp}_{\mathbf{w}_{k-1}}\mathbf{w}_k/\|\mathbf{w}_k\|_2\|_2^2$ is selected.

In the above WORD algorithm, only two candidates (i.e., β_a and β_b) are available for the parameter β_k, and both of them are real-valued. In fact, there exist complex-valued β_ks leading to the same response level at θ_k as that of the real-valued β_a or β_b in (3). As a result, it is more reasonable to assign a complex-valued β_k in the WORD scheme. This leads to the complex-coefficient weight vector orthogonal decomposition (C^2-WORD) algorithm as presented next.

More specifically, given the previous weight vector $\mathbf{w}_{k-1}$, in order to adjust the array response level of θ_k to its desired level ρ_k, we propose to update the weight vector as

$$\mathbf{w}_k = [\mathbf{w}_{\perp} \quad \mathbf{w}_{\parallel}][1 \quad \beta_k]^{\mathrm{T}}, \ \beta_k \in \mathbb{C}. \tag{6}$$

Different from the weight vector update of WORD in (1), the parameter β_k in (6) is complex-valued but not limited to be real-valued, although we have designated an identical notation (i.e., β_k).

To further obtain the trajectory of all the qualified β_ks satisfying the prescribed array response control requirement, we substitute (6) into $L_k(\theta_k,\theta_0)=\rho_k$ and obtain $\mathbf{z}_k^{\mathrm{H}}\mathbf{B}_k\mathbf{z}_k = 0$, where $\mathbf{z}_k \triangleq [1 \quad \beta_k]^{\mathrm{T}}$, $\mathbf{B}_k$ is a 2×2 Hermitian matrix given

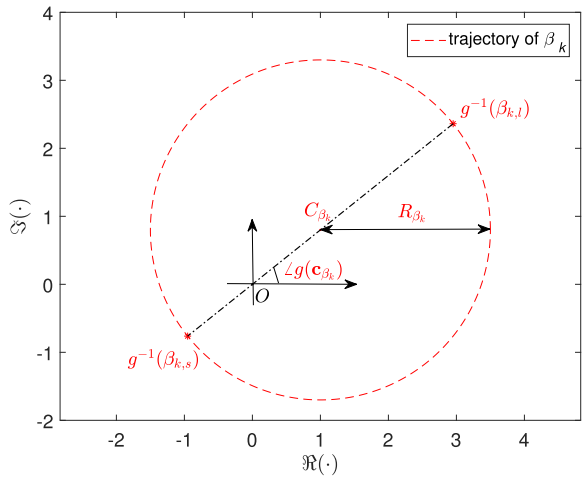

Fig. 1. Geometrical distribution of β_k in complex plane.

in (4). After some calculation, it is not hard to derive that the trajectory set of β_k in (6) is a circle $\mathbb{C}_{\beta_k}$

$$\mathbb{C}_{\beta_k} = \{\beta_k | \|[\Re(\beta_k), \Im(\beta_k)]^{\mathrm{T}} - \mathbf{c}_{\beta_k}\|_2 = R_{\beta_k}\} \tag{7}$$

with center

$$\mathbf{c}_{\beta_k} = \frac{1}{\mathbf{B}_k(2,2)} \begin{bmatrix} -\Re\left(\mathbf{B}_k(1,2)\right) \\ \Im\left(\mathbf{B}_k(1,2)\right) \end{bmatrix} \tag{8}$$

and radius

$$R_{\beta_k} = \sqrt{-\det(\mathbf{B}_k)} \big/ |\mathbf{B}_k(2,2)|. \tag{9}$$

Fig. 1 presents a geometric interpretation of the above result. One can see that the existing WORD algorithm selects the parameter β_k from the real-valued elements of $\mathbb{C}_{\beta_k}$. For C^2-WORD, we have extended the feasible set to complex domain. By doing so, the resulting performance may be improved, since it is possible to select a more appropriate β_k that may not be real-valued.

Moreover, the trajectory set of β_k in (7) indicates that there exist infinitely many solutions of (complex-valued) β_k adjusting the array response level of θ_k to its desired value ρ_k. To select an optimal $\beta_{k,\triangleright}$, we take the WNG into consideration and formulate the following constrained problem as

$$\max_{\beta_k} G(\mathbf{w}_k) = \frac{\left|\mathbf{w}_k^{\mathrm{H}}\mathbf{a}(\theta_0)\right|^2}{\|\mathbf{w}_k\|_2^2} \tag{10a}$$

$$\text{s.t. } \mathbf{w}_k = [\mathbf{w}_\perp \quad \mathbf{w}_\parallel][1 \quad \beta_k]^{\mathrm{T}} \tag{10b}$$

$$\beta_k \in \mathbb{C}_{\beta_k} \tag{10c}$$

where $G(\mathbf{w}_k)$ represents the corresponding WNG of the weight vector $\mathbf{w}_k$, $\mathbb{C}_{\beta_k}$ is given in (7). Although the problem (10) is nonconvex, its optimal solution can be analytically expressed as

$$\beta_{k,\triangleright} = \beta_{k,l} \triangleq \arg \max_{\beta_k \in \mathbb{C}_{\beta_k}} |\beta_k| = (|\mathbf{c}_{\beta_k}| + R_{\beta_k}) e^{j\angle g(\mathbf{c}_{\beta_k})} \tag{11}$$

see appendix A for the derivations. In (11), $g(\cdot)$ is a function satisfying $g(\mathbf{c}) = \mathbf{c}(1) + j\mathbf{c}(2)$ for a 2-D input vector, see $g^{-1}(\beta_{k,l})$ in Fig. 1 for the location of the optimal $\beta_{k,\triangleright}$.

Algorithm 1 C^2-WORD Algorithm

1: prescribe beam axis θ_0 and index k, give the previous weight vector $\mathbf{w}_{k-1}$, direction θ_k and the corresponding desired level ρ_k
2: determine the optimal $\beta_{k,\triangleright}$ in (11)
3: output the new weight vector $\mathbf{w}_k$ in (12)

Once the optimal $\beta_{k,\triangleright}$ is determined, we can express the ultimate weight vector of C^2-WORD as

$$\mathbf{w}_k = [\mathbf{w}_\perp \quad \mathbf{w}_\parallel][1 \quad \beta_{k,\triangleright}]^{\mathrm{T}}. \tag{12}$$

The above C^2-WORD algorithm results in small pattern variations on the uncontrolled angles, and performs at least as good as the state-of-the-art WORD approach. More importantly, the C^2-WORD algorithm plays a fundamental role in the later discussions. To make it clear, we summarize the C^2-WORD algorithm in Algorithm 1.

B. Formulation of Robust Sidelobe Control

The C^2-WORD algorithm developed in Section II-A can control the array response level of a given point in the absence of steering vector uncertainties. To realize array response control in the case when steering vector suffers from perturbation, we next formulate the problem of robust sidelobe control. For the convenience of later derivations, we first define the normalized magnitude response as

$$V_a(\theta) = |\mathbf{w}^{\mathrm{H}}\mathbf{a}(\theta)| / |\mathbf{w}^{\mathrm{H}}\mathbf{a}(\theta_0)|. \tag{13}$$

Note that the above $V_a(\theta)$ is different from the normalized power response $L(\theta, \theta_0)$ defined in Section II-A. One can readily find that $V_a^2(\theta) = L(\theta, \theta_0)$.

Clearly, $V_a(\theta)$ describes the array magnitude response in the absence of array uncertainties. In practice, however, the steering vector is usually influenced by the antenna array imperfections, such as, gain-phase mismatch, element position mismatch, mutual coupling effect, and so on. In this case, the actual steering vector, denoted by $\mathbf{b}(\theta)$, is given by

$$\mathbf{b}(\theta) = \mathbf{a}(\theta) + \Delta(\theta) \tag{14}$$

where $\Delta(\theta)$ is the unknown steering vector uncertainty that can be varied with θ. The actual normalized magnitude response, denoted by $V_b(\theta)$, can be expressed as

$$V_b(\theta) = |\mathbf{w}^{\mathrm{H}}\mathbf{b}(\theta)| / |\mathbf{w}^{\mathrm{H}}\mathbf{b}(\theta_0)| \tag{15}$$

which is different from $V_a(\theta)$ under normal circumstances. Note that in (15), we keep on using the beamformer output of θ_0 as the normalization factor, although the actual beam axis may have deviated slightly from θ_0 due to the influence of steering vector uncertainties. In robust sidelobe control, we consider how to make the actual magnitude response $V_b(\theta)$ lower than specific levels in certain sidelobe regions.

C. Boundary Analysis on Array Response

To proceed, we first present a boundary analysis on the actual magnitude response $V_b(\theta)$. To do so, we reasonably assume that the uncertainty $\Delta(\theta)$ is norm-bounded as

$$\|\Delta(\theta)\|_2 \le \varepsilon(\theta) \tag{16}$$

where $\varepsilon(\theta)$ is a known constant at θ. Then, according to the triangle inequality property, we have

$$\begin{aligned} |\mathbf{w}^{\mathrm{H}}\mathbf{b}(\theta)| &= |\mathbf{w}^{\mathrm{H}}(\mathbf{a}(\theta)+\Delta(\theta))| \\ &\le |\mathbf{w}^{\mathrm{H}}\mathbf{a}(\theta)| + |\mathbf{w}^{\mathrm{H}}\Delta(\theta)| \\ &\le |\mathbf{w}^{\mathrm{H}}\mathbf{a}(\theta)| + \|\mathbf{w}\|_2 \cdot \|\Delta(\theta)\|_2 \\ &\le |\mathbf{w}^{\mathrm{H}}\mathbf{a}(\theta)| + \varepsilon(\theta)\|\mathbf{w}\|_2. \end{aligned} \tag{17}$$

Similarly

$$\begin{aligned} |\mathbf{w}^{\mathrm{H}}\mathbf{b}(\theta)| &= |\mathbf{w}^{\mathrm{H}}(\mathbf{a}(\theta)+\Delta(\theta))| \\ &\ge |\mathbf{w}^{\mathrm{H}}\mathbf{a}(\theta)| - |\mathbf{w}^{\mathrm{H}}\Delta(\theta)| \\ &\ge |\mathbf{w}^{\mathrm{H}}\mathbf{a}(\theta)| - \|\mathbf{w}\|_2 \cdot \|\Delta(\theta)\|_2 \\ &\ge |\mathbf{w}^{\mathrm{H}}\mathbf{a}(\theta)| - \varepsilon(\theta)\|\mathbf{w}\|_2. \end{aligned} \tag{18}$$

Combining (17) and (18), one can readily find that

$$\begin{aligned} V_b(\theta) &= \frac{|\mathbf{w}^{\mathrm{H}}(\mathbf{a}(\theta)+\Delta(\theta))|}{|\mathbf{w}^{\mathrm{H}}(\mathbf{a}(\theta_0)+\Delta(\theta_0))|} \\ &\le \frac{|\mathbf{w}^{\mathrm{H}}\mathbf{a}(\theta)| + \varepsilon(\theta)\|\mathbf{w}\|_2}{|\mathbf{w}^{\mathrm{H}}\mathbf{a}(\theta_0)| - \varepsilon(\theta_0)\|\mathbf{w}\|_2} \\ &= \frac{V_a(\theta) + \varepsilon(\theta)\cdot\|\mathbf{w}\|_2/|\mathbf{w}^{\mathrm{H}}\mathbf{a}(\theta_0)|}{1 - \varepsilon(\theta_0)\cdot\|\mathbf{w}\|_2/|\mathbf{w}^{\mathrm{H}}\mathbf{a}(\theta_0)|} \\ &\triangleq V_u(\theta) \end{aligned} \tag{19}$$

and

$$\begin{aligned} V_b(\theta) &\ge \frac{|\mathbf{w}^{\mathrm{H}}\mathbf{a}(\theta)| - \varepsilon(\theta)\|\mathbf{w}\|_2}{|\mathbf{w}^{\mathrm{H}}\mathbf{a}(\theta_0)| + \varepsilon(\theta_0)\|\mathbf{w}\|_2} \\ &= \frac{V_a(\theta) - \varepsilon(\theta)\cdot\|\mathbf{w}\|_2/|\mathbf{w}^{\mathrm{H}}\mathbf{a}(\theta_0)|}{1 + \varepsilon(\theta_0)\cdot\|\mathbf{w}\|_2/|\mathbf{w}^{\mathrm{H}}\mathbf{a}(\theta_0)|} \\ &\triangleq V_l(\theta). \end{aligned} \tag{20}$$

Compactly, we have

$$0 \le V_l(\theta) \le V_b(\theta) \le V_u(\theta) \tag{21}$$

where $V_u(\theta)$ and $V_l(\theta)$ stand for the worst-case upper and lower boundaries of magnitude response, respectively. According to (21), the actual response $V_b(\theta)$ fluctuates in the range $[V_l(\theta), V_u(\theta)]$. In addition, it should be noted that we have implicitly assumed in (19) that

$$|\mathbf{w}^{\mathrm{H}}\mathbf{a}(\theta_0)| - \varepsilon(\theta_0)\|\mathbf{w}\|_2 > 0. \tag{22}$$

Otherwise, it leads to $V_u(\theta) < 0$ and (19) does not hold true.

D. Formulation of Robust One-Point Sidelobe Control

In Section II-C, a boundary analysis on the array response is presented. We next formulate the problem of robust one-point sidelobe control, i.e., making the response level of a given sidelobe point lower than a specific value in the presence of steering vector uncertainties.

More specifically, denote the desired magnitude upper beampattern by $V_d(\theta)$. Give a previous weight vector $\mathbf{w}_{k-1}$ and a sidelobe angle θ_k to be controlled, where the subscript k is the step index. It is required to find a new weight vector $\mathbf{w}_k$ that makes the actual (magnitude) response level of θ_k lower than $V_d(\theta_k)$. To simplify notations, in sequel, we follow the usages of $V_a(\theta)$, $V_b(\theta)$, $V_u(\theta)$ and $V_l(\theta)$ defined in the two preceding sections, and designate them to stand for the counterparts of $\mathbf{w}_k$. Then, the problem of one-point robust sidelobe control can be formulated as

$$\text{find } \mathbf{w}_k \tag{23a}$$

$$\text{s.t } V_b(\theta_k) \le V_d(\theta_k). \tag{23b}$$

Note that there exist unknown perturbations on the steering vector [see (14)]. As a result, it is not easy to adjust $V_b(\theta_k)$ as desired.

To tackle problem (23), we recall (21) and formulate a conservative version of (23) as

$$\text{find } \mathbf{w}_k \tag{24a}$$

$$\text{s.t } V_u(\theta_k) \le V_d(\theta_k) \tag{24b}$$

where the maximum possible response level at θ_k [i.e., $V_u(\theta_k)$] is restricted to be lower than $V_d(\theta_k)$. Since $V_b(\theta_k)$ is not greater than $V_u(\theta_k)$, one learns that the original constraint (23b) is satisfied if only (24b) is true.

One possible way to make the constraint (24b) qualified is to take $V_u(\theta_k)$ as its minimum value, which may be close to zero. By doing so, the actual response $V_b(\theta_k)$ would also approach to zero because of the constraint (21). As a result, it may broaden the main lobe of $V_b(\theta)$ and/or lower the resulting WNG. To alleviate this drawback, a high value of $V_b(\theta_k)$ is expected under the condition that (24b) is satisfied. As aforementioned, $V_b(\theta_k)$ fluctuates in the range $[V_l(\theta_k), V_u(\theta_k)]$. Then, a reasonable way to elevate $V_b(\theta_k)$ is to lift both the lower boundary response level $V_l(\theta_k)$ and the upper boundary response level $V_u(\theta_k)$. According to (24b), the maximum of $V_u(\theta_k)$ is $V_d(\theta_k)$, and we can improve the general level of $V_b(\theta_k)$ by fixing $V_u(\theta_k)$ as $V_d(\theta_k)$ and then solve the following optimization problem:

$$\max_{\mathbf{w}_k} \ V_l(\theta_k) \tag{25a}$$

$$\text{s.t. } V_u(\theta_k) = V_d(\theta_k). \tag{25b}$$

For the given $V_a(\theta_k)$, $\varepsilon(\theta_0)$, and $\varepsilon(\theta_k)$, it is not hard to observe from (19) and (20) that

$$V_u(\theta_k) - V_l(\theta_k) \propto \frac{\|\mathbf{w}_k\|_2}{\left|\mathbf{w}_k^{\mathrm{H}}\mathbf{a}(\theta_0)\right|}. \tag{26}$$

Thus, one can reformulate problem (25) as

$$\max_{\mathbf{w}_k} \ G(\mathbf{w}_k) = \frac{\left|\mathbf{w}_k^{\mathrm{H}}\mathbf{a}(\theta_0)\right|^2}{\|\mathbf{w}_k\|_2^2} \tag{27a}$$

$$\text{s.t. } V_u(\theta_k) = V_d(\theta_k) \tag{27b}$$

where $G(\mathbf{w}_k)$ stands for the WNG in the absence of steering vector uncertainties, and has also been used in problem (10) in Section II-A. Since $\|\mathbf{w}_k\|_2/|\mathbf{w}_k^{\mathrm{H}}\mathbf{a}(\theta_0)|$ is directly proportional to the pattern perturbations, i.e., $V_u(\theta_k) - V_a(\theta_k)$ and

$V_a(\theta_k) - V_l(\theta_k)$, the solution of problem (27) results in small pattern perturbations for the given $\varepsilon(\theta_0)$ and $\varepsilon(\theta_k)$.

Recalling the definition of $V_u(\theta_k)$ in (19), we can reformulate the robust one-point sidelobe control problem (27) as

$$\max_{\mathbf{w}_k} \; G(\mathbf{w}_k) = \frac{\left|\mathbf{w}_k^{\mathrm{H}}\mathbf{a}(\theta_0)\right|^2}{\|\mathbf{w}_k\|_2^2} \tag{28a}$$

$$\text{s.t. } V_a(\theta_k) = V_{\mathbf{w}}(\theta_k) \tag{28b}$$

where $V_{\mathbf{w}}(\theta)$ is defined as

$$V_{\mathbf{w}}(\theta) \triangleq V_d(\theta) - \gamma(\theta)\|\mathbf{w}_k\|_2 / \left|\mathbf{w}_k^{\mathrm{H}}\mathbf{a}(\theta_0)\right| \tag{29}$$

with $\gamma(\theta) \triangleq V_d(\theta)\varepsilon(\theta_0) + \varepsilon(\theta)$. Clearly, the nonconvex problem (28) maximizes WNG with specific constraint on the (ideal) response level at θ_k. This is similar to the response control problem in the absence of steering vector uncertainties, as formulated in Section II-A. Nevertheless, different from the array response control problem discussed in Section II-A, it should be noted that the right side of the constraint (28b), i.e., $V_{\mathbf{w}}(\theta_k)$, depends on the optimization variable $\mathbf{w}_k$ as well. In addition, the previous weight vector $\mathbf{w}_{k-1}$ is not taken into consideration in the formulating problem (28). As a result, it may lead to large pattern variations at the uncontrolled points, comparing to the previous beampattern response. Recalling that the C^2-WORD scheme devised in Section II-A maximizes WNG and results in small pattern variations, it provides some inspiration to use C^2-WORD algorithm to realize one-point sidelobe control, as detailed in the next section.

E. Robust C^2-WORD Algorithm

In this section, we propose a new method to realize robust one-point sidelobe control and name it as robust C^2-WORD algorithm. The devised algorithm is built on the foundation of the C^2-WORD scheme developed in Section II-A. More importantly, it offers an analytical expression for the new weight vector $\mathbf{w}_k$ and results in small pattern variations at the uncontrolled points.

To begin with, we recall C^2-WORD scheme in Section II-A, and incorporate a new constraint into (28) as

$$\max_{\beta_k} \; G(\mathbf{w}_k) \tag{30a}$$

$$\text{s.t. } V_a(\theta_k) = V_{\mathbf{w}}(\theta_k) \tag{30b}$$

$$\mathbf{w}_k = [\mathbf{w}_\perp \quad \mathbf{w}_\parallel][1 \quad \beta_k]^{\mathrm{T}}, \; \beta_k \in \mathbb{C} \tag{30c}$$

where the constraint of orthogonal decomposition has been added in (30c). Once the optimal $\beta_{k,\star}$ of (30) is obtained, we can express the ultimate weight vector $\mathbf{w}_k$ as

$$\mathbf{w}_k = [\mathbf{w}_\perp \quad \mathbf{w}_\parallel][1 \quad \beta_{k,\star}]^{\mathrm{T}}. \tag{31}$$

It should be emphasized that the resulting weight vector (31) may not be the global optimal solution of problem (28), since we have assigned a new constraint in problem (30). In spite of that, we will show later that the obtained $\mathbf{w}_k$ in (31) performs well on robust sidelobe control with small pattern variations at the uncontrolled points. The remaining problem is how to determine the optimal $\beta_{k,\star}$ of (30), as presented next.

For the sake of subsequent convenience, we first define

$$\rho_a \triangleq V_a^2(\theta_k) \tag{32}$$

which represents the resulting ideal power response level at θ_k. Then, for the given θ_0, θ_k, $\mathbf{w}_{k-1}$, $V_d(\theta_k)$, $\varepsilon(\theta_0)$ and $\varepsilon(\theta_k)$, we can indirectly determine the optimal $\beta_{k,\star}$ by finding the corresponding ρ_a when problem (30) is solved.

After some calculation, one can see that the ultimate ρ_a in problem (30) satisfies the following quartic polynomial:

$$A^2\rho_a^4 + (2AC - B^2)\rho_a^3 + (2AE - 2BD + C^2)\rho_a^2 + (2CE - D^2)\rho_a + E^2 = 0. \tag{33}$$

The derivation of (33) is presented in appendix B, where the expressions of A, B, C, D, E are also specified [see (79)]. In fact, there are four candidates of ρ_a satisfying (33), and they can be analytically expressed; see the following lemma to find their specific expressions.

Lemma 1: The four roots x_i $(i = 1, 2, 3, 4)$ for the following general quartic equation:

$$ax^4 + bx^3 + cx^2 + dx + e = 0, \;\; (a \neq 0) \tag{34}$$

are given by

$$x_1 = -\frac{b}{4a} + S + \frac{\sqrt{-4S^2 - 2p - \frac{q}{S}}}{2} \tag{35a}$$

$$x_2 = -\frac{b}{4a} + S - \frac{\sqrt{-4S^2 - 2p - \frac{q}{S}}}{2} \tag{35b}$$

$$x_3 = -\frac{b}{4a} - S + \frac{\sqrt{-4S^2 - 2p + \frac{q}{S}}}{2} \tag{35c}$$

$$x_4 = -\frac{b}{4a} - S - \frac{\sqrt{-4S^2 - 2p + \frac{q}{S}}}{2} \tag{35d}$$

where

$$p \triangleq \frac{8ac - 3b^2}{8a^2} \tag{36a}$$

$$q \triangleq \frac{b^3 - 4abc + 8a^2d}{8a^3} \tag{36b}$$

$$S \triangleq \frac{\sqrt{-\frac{2}{3}p + \frac{1}{3a}\left(Q + \frac{\zeta_0}{Q}\right)}}{2} \tag{36c}$$

with

$$Q \triangleq \sqrt[3]{\left(\zeta_1 + \sqrt{\zeta_1^2 - 4\zeta_0^3}\right)/2} \tag{37a}$$

$$\zeta_0 \triangleq c^2 - 3bd + 12ae \tag{37b}$$

$$\zeta_1 \triangleq 2c^3 - 9bcd + 27b^2e + 27ad^2 - 72ace. \tag{37c}$$

Proof: See [25]. ∎

According to (35) in Lemma 1, we can obtain the four solutions of quartic equation (33), and denote them as $\rho_{a,1}, \rho_{a,2}, \rho_{a,3}, \rho_{a,4}$, respectively. Recalling our previous discussions, we note that the qualified ρ_a is real-valued and satisfies

$$\rho_a \in \left[0, V_d^2(\theta_k)\right). \tag{38}$$

Algorithm 2 Robust C^2-WORD Algorithm

1: prescribe beam axis θ_0 and index k, give the previous weight vector $\mathbf{w}_{k-1}$, sidelobe angle θ_k, the desired (mag nitude) upper response level $V_d(\theta_k)$ and the steering vector uncertainty boundaries $\varepsilon(\theta_0)$ and $\varepsilon(\theta_k)$
2: construct quartic equation (33) and find its solutions (i.e., $\rho_{a,1}$, $\rho_{a,2}$, $\rho_{a,3}$, $\rho_{a,4}$) according to Lemma 1
3: determine the ultimate $\rho_{a,\star}$ by solving problem (39)
4: apply C^2-WORD algorithm to adjust the ideal array response level of θ_k to $\rho_{a,\star}$, see Algorithm 1
5: output the new weight vector $\mathbf{w}_k$ in (31)

In addition, recalling the expression of $V_{\mathbf{w}}(\theta)$ in (29), one can readily know that ρ_a is directly proportional to $G(\mathbf{w}_k)$. Thus, we can determine the optimal $\rho_{a,\star}$ by solving the following simple problem:

$$\max_{\rho_a} \ \rho_a \tag{39a}$$
$$\text{s.t. } \rho_a \in \{\rho_{a,1}, \rho_{a,2}, \rho_{a,3}, \rho_{a,4}\} \tag{39b}$$
$$\rho_a \in [0, V_d^2(\theta_k)). \tag{39c}$$

Once the optimal $\rho_{a,\star}$ is determined, we can remove the constraint (30b) and reformulate the problem (30) as

$$\max_{\beta_k} \ G(\mathbf{w}_k) \tag{40a}$$
$$\text{s.t. } L_k(\theta_k, \theta_0) = \rho_{a,\star} \tag{40b}$$
$$\mathbf{w}_k = [\mathbf{w}_\perp \ \ \mathbf{w}_\parallel][1 \ \ \beta_k]^{\mathrm{T}}, \quad \beta_k \in \mathbb{C}. \tag{40c}$$

The above problem (40) has an analytical solution, see problem (10) and (11) in Section II-A for details. Thus, we obtained the ultimate $\beta_{k,\star}$ and its corresponding weight vector $\mathbf{w}_k$ in (31). This completes the robust one-point response control at a given sidelobe point. Finally, we summarize the proposed robust C^2-WORD algorithm in Algorithm 2.

F. Restriction Between $V_d(\theta_k)$ and $\varepsilon(\theta_k)$

In Section II-E, we use the C^2-WORD scheme to realize robust sidelobe control at a preassigned angle θ_k. It should be pointed out that there exists an implicit restriction between the minimum reachable upper response level $V_d(\theta_k)$ and the steering vector uncertainty norm boundary $\varepsilon(\theta_k)$, as investigated next.

To begin with, we note that $V_a(\theta_k) \geq 0$. Since $V_a(\theta_k)$ is generally in proportional to $V_u(\theta_k)$, we can obtain the minimum reachable level of $V_d(\theta_k)$ [denoted as $\overline{V}_d(\theta_k)$] by setting $V_a(\theta_k) = 0$. Recalling (29) and (30b), $\overline{V}_d(\theta_k)$ is given by

$$\begin{aligned}\overline{V}_d(\theta_k) &= \gamma(\theta_k)\|\mathbf{w}_k\|_2 / \left|\mathbf{w}_k^{\mathrm{H}}\mathbf{a}(\theta_0)\right| \\ &= (\overline{V}_d(\theta_k)\varepsilon(\theta_0) + \varepsilon(\theta_k)) \cdot \|\mathbf{w}_k\|_2 / \left|\mathbf{w}_k^{\mathrm{H}}\mathbf{a}(\theta_0)\right| \\ &= (\overline{V}_d(\theta_k)\varepsilon(\theta_0) + \varepsilon(\theta_k)) \cdot \|\mathbf{w}_\perp\|_2 / \left|\mathbf{w}_\perp^{\mathrm{H}}\mathbf{a}(\theta_0)\right| \end{aligned} \tag{41}$$

where we have utilized the fact that $\beta_\star = 0$ and $\mathbf{w}_k = \mathbf{w}_\perp$ when $V_a(\theta_k) = 0$ applies. According to (41), $V_d(\theta_k)$ should be taken to satisfy

$$V_d(\theta_k) \geq \overline{V}_d(\theta_k) = \frac{\varepsilon(\theta_k)\|\mathbf{w}_\perp\|_2}{\left|\mathbf{w}_\perp^{\mathrm{H}}\mathbf{a}(\theta_0)\right| - \varepsilon(\theta_0)\|\mathbf{w}_\perp\|_2} \tag{42}$$

which specifies the restriction between $V_d(\theta_k)$ and $\varepsilon(\theta_k)$ for the given $\varepsilon(\theta_0)$ and $\mathbf{a}(\theta_0)$. Clearly, the lesser $\varepsilon(\theta_k)$ is, the lower level $V_d(\theta_k)$ can be taken.

Note from (42) that the minimum reachable level of $V_d(\theta_k)$ [i.e, $\overline{V}_d(\theta_k)$] depends on the previous weight vector $\mathbf{w}_{k-1}$ as well. Utilizing the Cauchy–Schwarz inequality that $\|\mathbf{w}_\perp\|_2\|\mathbf{a}(\theta_0)\|_2 \geq |\mathbf{w}_\perp^{\mathrm{H}}\mathbf{a}(\theta_0)|$, one can further obtain

$$V_d(\theta_k) \geq \overline{V}_d(\theta_k) \geq \frac{\varepsilon(\theta_k)}{\|\mathbf{a}(\theta_0)\|_2 - \varepsilon(\theta_0)} \triangleq \chi(\theta_k) \tag{43}$$

where the introduced $\chi(\theta_k)$ is independent of the previous weight vector and specifies a lower boundary of $\overline{V}_d(\theta_k)$. Note that the resulting $\chi(\theta_k)$ in (43) measures a general value of the minimum achievable level of $V_d(\theta_k)$, although it may not be reached for an arbitrarily specified previous weight $\mathbf{w}_{k-1}$.

In addition, according to the observation in (42), we know that there always exists a qualified solution $\check{\rho}_a$ for (33) falling within the range $[0, V_d^2(\theta_k))$ [as formulated in (38)], provided that

$$V_d(\theta_k) \geq \frac{\varepsilon(\theta_k)\|\mathbf{w}_\perp\|_2}{\left|\mathbf{w}_\perp^{\mathrm{H}}\mathbf{a}(\theta_0)\right| - \varepsilon(\theta_0)\|\mathbf{w}_\perp\|_2}. \tag{44}$$

See appendix C for the derivations. If the value of $V_d(\theta_k)$ is too small [for example, smaller than $\chi(\theta_k)$ in (43)], it is not guaranteed to obtain a qualified ρ_a falling within the range $[0, V_d^2(\theta_k))$.

III. Practical Consideration

In Section II, a robust C^2-WORD algorithm is devised to adjust the response level of a preassigned sidelobe point in the presence of steering vector perturbation. As aforementioned, the steering vector uncertainty $\Delta(\theta)$ is assumed to be norm-bounded by a known constant $\varepsilon(\theta)$. To enhance the practicality of the robust C^2-WORD algorithm, we next consider how to determine $\Delta(\theta)$ and the corresponding $\varepsilon(\theta)$ in practical applications with some reasonable assumptions.

In this paper, we assume that the array suffers from channel gain-phase mismatch, element position mismatch, mutual coupling effect, or their superpositions. On this basis, we can model the actual steering vector $\mathbf{b}(\theta)$ in (14) as

$$\mathbf{b}(\theta) = \mathbf{C}(\theta)\mathbf{a}(\theta) = \mathbf{a}(\theta) + \underbrace{[\mathbf{C}(\theta) - \mathbf{I}]\mathbf{a}(\theta)}_{\Delta(\theta)} \tag{45}$$

where $\mathbf{C}(\theta)$ is a certain matrix whose elements may vary with θ. Let us define

$$\mathbf{E}(\theta) \triangleq \mathbf{C}(\theta) - \mathbf{I}. \tag{46}$$

Then according to (45), we have $\Delta(\theta) = \mathbf{E}(\theta)\mathbf{a}(\theta)$, from which one can further derive that

$$\|\Delta(\theta)\|_2 = \|\mathbf{E}(\theta)\mathbf{a}(\theta)\|_2 \leq \|\mathbf{E}(\theta)\|_2\|\mathbf{a}(\theta)\|_2 \tag{47}$$

where $\|\mathbf{E}(\theta)\|_2$ is the spectral matrix norm [26] of $\mathbf{E}(\theta)$ satisfying

$$\|\mathbf{E}(\theta)\|_2 = \sqrt{\lambda_{\max}(\mathbf{E}^{\mathrm{H}}(\theta)\mathbf{E}(\theta))}. \tag{48}$$

Clearly, if $\mathbf{E}(\theta)$ is known or can be estimated, we can set the corresponding $\varepsilon(\theta)$ in (16) as

$$\varepsilon(\theta) = \|\mathbf{E}(\theta)\|_2\|\mathbf{a}(\theta)\|_2. \tag{49}$$

However, this is not a common occurrence, since $\mathbf{E}(\theta)$ [or $\mathbf{C}(\theta)$] is usually a random matrix with certain statistical model for its entries [27]. In this case, we can determine $\varepsilon(\theta)$ by

$$\varepsilon(\theta) = \|\mathbf{a}(\theta)\|_2 \cdot \max \|\mathbf{E}(\theta)\|_2. \tag{50}$$

We next present some specific scenarios, in which the steering vector uncertainty boundary $\varepsilon(\theta)$ can be analytically expressed according to (50). For the sake of simplicity, we only consider linear arrays, although the extension to more complicated configurations are straightforward.

A. Channel Gain-Phase Mismatch

To begin with, we consider the channel gain-phase mismatch [28]–[30]. In this case, we have

$$\mathbf{C}(\theta) = \mathrm{Diag}([1, g_2 e^{j\varphi_2}, \ldots, g_N e^{j\varphi_N}]) \tag{51}$$

where g_n and φ_n stand for the channel gain and phase error of the nth element, respectively, $n = 2, \ldots, N$. Note that the measurements have been normalized by that of the first element. Accordingly, $\mathbf{E}(\theta)$ can be expressed as

$$\mathbf{E}(\theta) = \mathrm{Diag}([0, g_2 e^{j\varphi_2} - 1, \ldots, g_N e^{j\varphi_N} - 1]). \tag{52}$$

Recalling (48), one can readily obtain that

$$\max \|\mathbf{E}(\theta)\|_2 = \max_{n=2,\ldots,N} |g_n e^{j\varphi_n} - 1|. \tag{53}$$

Suppose that g_n and φ_n are randomly distributed in certain regions as

$$g_n \in [g_{n,l}, g_{n,u}], \quad \varphi_n \in [\varphi_{n,l}, \ \varphi_{n,u}], \ n = 2, \ldots, N \tag{54}$$

where g_l, g_u, φ_l and φ_u stand for the corresponding boundaries. Then, we can obtain from (53) that

$$\max \|\mathbf{E}(\theta)\|_2 = \max_{n\in\{2,\ldots,N\},\tau\in\{l,u\},\varsigma\in\{l,u\}} |g_{n,\tau} e^{j\varphi_{n,\varsigma}} - 1| \triangleq \delta_1.$$

According to (50), one can set $\varepsilon(\theta)$ as

$$\varepsilon(\theta) = \|\mathbf{a}(\theta)\|_2 \cdot \delta_1. \tag{55}$$

B. Element Position Mismatch

We next analyze the steering vector uncertainty $\Delta(\theta)$ and determine its corresponding $\varepsilon(\theta)$ in the presence of element position uncertainties [31]. In this case, $\mathbf{C}(\theta)$ is given by

$$\mathbf{C}(\theta) = \mathrm{Diag}([1, e^{j2\pi\alpha_2 \sin(\theta)/\lambda}, \ldots, e^{j2\pi\alpha_N \sin(\theta)/\lambda}]) \tag{56}$$

where λ stands for wavelength, α_n represents the position deviation of the nth element from its ideal location d_n, $n = 2, \ldots, N$. According to (46), one can express $\mathbf{E}(\theta)$ as

$$\mathbf{E}(\theta) = \mathrm{Diag}([0, e^{j2\pi\alpha_2 \sin(\theta)/\lambda} - 1, \ldots, e^{j2\pi\alpha_N \sin(\theta)/\lambda} - 1]).$$

Suppose that α_n is randomly distributed in the range as

$$\alpha_n \in [\alpha_{n,l}, \alpha_{n,u}], \ n = 2, \ldots, N \tag{57}$$

where $\alpha_{n,l}$ and $\alpha_{n,u}$ are known boundaries. Then, we can obtain the following result about $\mathbf{E}(\theta)$, that is,

$$\max \|\mathbf{E}(\theta)\|_2 = \max_{n\in\{2,\ldots,N\},\tau\in\{l,u\}} |e^{j2\pi\alpha_{n,\tau} \sin(\theta)/\lambda} - 1| \triangleq \delta_2(\theta).$$

Different from the δ_1 in Section III-A, the above $\delta_2(\theta)$ is directionally dependent. Finally, according to (50), we can set $\varepsilon(\theta)$ as

$$\varepsilon(\theta) = \|\mathbf{a}(\theta)\|_2 \cdot \delta_2(\theta). \tag{58}$$

C. Mutual Coupling Effect

Now we consider the steering vector uncertainty arising from mutual coupling effect [32]–[34]. Following [27], we only consider the electromagnetic coupling between adjacent elements of a linear array, and express the mutual coupling matrix $\mathbf{C}(\theta)$ as

$$\mathbf{C}(\theta) = \begin{bmatrix} 1 & \xi \cdot z_{1,2} & 0 & \cdots & 0 \\ \xi \cdot z_{2,1} & 1 & \xi \cdot z_{2,3} & \ddots & \vdots \\ 0 & \xi \cdot z_{3,2} & 1 & \ddots & 0 \\ \vdots & \ddots & \ddots & 1 & \xi \cdot z_{N-1,N} \\ 0 & \cdots & 0 & \xi \cdot z_{N,N-1} & 1 \end{bmatrix}$$

which is complex symmetry. In $\mathbf{C}(\theta)$, ξ is the known coupling level between channels, $z_{i,j}$ are random variables with a fixed magnitude $|z_{i,j}| = 1$. It should be noted that only the value of coupling level ξ is needed in our discussion, and the measurements or exact values of $z_{i,j}$s are not necessary for us. This makes the study different from that in [9], where the whole coupling matrix $\mathbf{C}(\theta)$ has to be measured in advance. On this basis, we recall (46) and obtain that

$$\mathbf{E}(\theta) = \xi \cdot \begin{bmatrix} 0 & z_{1,2} & 0 & \cdots & 0 \\ z_{2,1} & 0 & z_{2,3} & \ddots & \vdots \\ 0 & z_{3,2} & 0 & \ddots & 0 \\ \vdots & \ddots & \ddots & 0 & z_{N-1,N} \\ 0 & \cdots & 0 & z_{N,N-1} & 0 \end{bmatrix}. \tag{59}$$

According to the Gershgorin circle theorem [35], that is,

$$|\lambda_{\max}(\mathbf{D})| \le \max_{p=1,\ldots,P} \sum_{l=1}^{L} |\mathbf{D}(p,l)| \tag{60}$$

where $\mathbf{D}$ is a $P \times L$ matrix, it can be concluded that

$$\max \|\mathbf{E}(\theta)\|_2 = \sqrt{\lambda_{\max}(\mathbf{E}^{\mathrm{H}}(\theta)\mathbf{E}(\theta))} \le 2\xi \triangleq \delta_3. \tag{61}$$

From (50), we can set $\varepsilon(\theta)$ as

$$\varepsilon(\theta) = \|\mathbf{a}(\theta)\|_2 \cdot \delta_3 = 2\xi \|\mathbf{a}(\theta)\|_2. \tag{62}$$

IV. Robust Sidelobe Synthesis

In this section, we introduce the application of robust C^2-WORD algorithm to sidelobe synthesis in the presence of steering vector imperfections. The general strategy is similar to the concept of pattern synthesis using WORD in [21]. However, different from the WORD approach, we realize robust sidelobe synthesis by successively adjusting the worst-case upper boundary magnitude pattern [i.e., $V_u(\theta)$], but not the ideal beampattern $V_a(\theta)$. For the sake of clarity, in sequel, we incorporate the subscript k into $V_a(\theta)$ and $V_u(\theta)$, and use

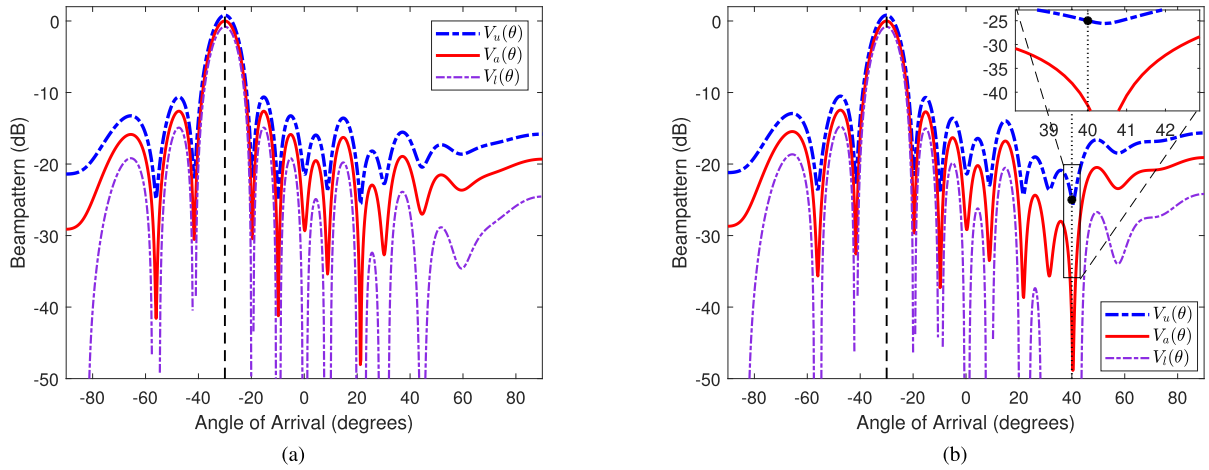

Fig. 2. Illustration of response control for a non-uniformly spaced linear array. (a) Before array response control. (b) After array response control.

Algorithm 3 Proposed Robust Sidelobe Synthesis Algorithm

give θ_0, $\varepsilon(\theta)$, the desired magnitude upper pattern $V_d(\theta)$, the initial weight vector $\mathbf{w}_0$ and its corresponding worst case upper boundary pattern $V_{u,0}(\theta)$, set $k = 1$
while 1 **do**
  select an angle θ_k by comparing $V_{u,k-1}(\theta)$ with $V_d(\theta)$
  apply robust C^2-WORD (see Algorithm 2) to realize $V_{u,k}(\theta_k) = V_d(\theta_k)$, obtain $\mathbf{w}_k$ in (31) and the corresponding upper boundary pattern $V_{u,k}(\theta)$
  if $V_{u,k}(\theta)$ is not satisfactory **then**
    set $k = k + 1$
  else
    break
  end if
end while
output $\mathbf{w}_k$

$V_{a,k}(\theta)$ and $V_{u,k}(\theta)$ to stand for the counterparts of the weight vector $\mathbf{w}_k$.

More precisely, an initial ideal pattern $V_{a,0}(\theta)$ and the corresponding worst-case upper boundary pattern $V_{u,0}(\theta)$ are firstly obtained from (13) and (19), respectively, by setting the initial weight vector as $\mathbf{w}_0$. Then, following the angle selection strategy in [21], we choose an angle θ_1, at which $V_{u,0}(\theta)$ has a peak point and deviates most from the desired upper pattern $V_d(\theta)$. Next, the robust C^2-WORD scheme is applied to modify the weight vector $\mathbf{w}_0$ to $\mathbf{w}_1$, by setting the output of $V_{u,1}(\theta_1)$ as $V_d(\theta_1)$. Similarly, by comparing $V_{u,1}(\theta)$ with $V_d(\theta)$, a second angle θ_2, at which the response is needed to be adjusted, is selected. An updated weight vector $\mathbf{w}_2$ can thus be obtained via robust C^2-WORD algorithm. The above procedure is carried out successively once the sidelobe responses of $V_{u,k}(\theta)$ are lower than $V_d(\theta)$. To make the above descriptions clear, we summarize the proposed robust sidelobe synthesis algorithm in Algorithm 3.

In practice, it is necessary to discretize the angular sector and only calculate the values of $V_{u,k}(\theta)$ on finite grid points. For different angular resolutions, there is a tradeoff between the performance of the robust C^2-WORD algorithm and its computational load. With a coarse discretization, it requires less searching points and thus lower computational load to finish the synthesis procedure. However, in the case when a low angular resolution applies, the selected point in each control step may not be a real sidelobe peak, and the resulting beampattern may be unsatisfactory. As a matter of fact, even using a dense angular discretization, the proposed robust C^2-WORD algorithm still runs faster than the conventional convex programming method in [8], as presented in the next section.

TABLE I
ELEMENT POSITIONS OF THE NONUNIFORM LINEAR ARRAY

n	$x_n(\lambda)$	n	$x_n(\lambda)$	n	$x_n(\lambda)$	n	$x_n(\lambda)$
1	0.00	4	1.55	7	3.05	10	4.55
2	0.45	5	2.10	8	3.65	11	5.05
3	1.00	6	2.60	9	4.10	12	5.50

V. NUMERICAL RESULTS

We next present some simulations to show the effectiveness of the proposed robust C^2-WORD scheme on array response control and pattern synthesis under various settings. To verify the superiority of our algorithm, the results of WORD algorithm in [21] and CP method in [8] are also presented if applicable. Unless otherwise specified, we take $\mathbf{a}(\theta_0)$ as the initial weight, and set the discretization interval of the angular observation sector $[-\pi/2, \pi/2]$ as 0.1°, in the implementations of both WORD and robust C^2-WORD. In addition, to result a weight vector with l_2 norm one, we normalize the ultimate weight vector in the following tests.

A. Illustration of Robust Sidelobe Control

In this section, we illustrate the performance of robust C^2-WORD on sidelobe control at a given point. In the first example, we consider a nonuniformly spaced linear array with 12 elements, see Table I for its element positions. The beam axis is steered to $\theta_0 = -30°$ and the norm boundary of steering vector uncertainty is taken as $\varepsilon(\theta) = 0.16$. In this case, it is required to adjust the (actual) sidelobe response at $\theta_1 = 40°$ to be lower than $V_d(\theta_1) = -25$ dB. Fig. 2(a) depicts the ideal

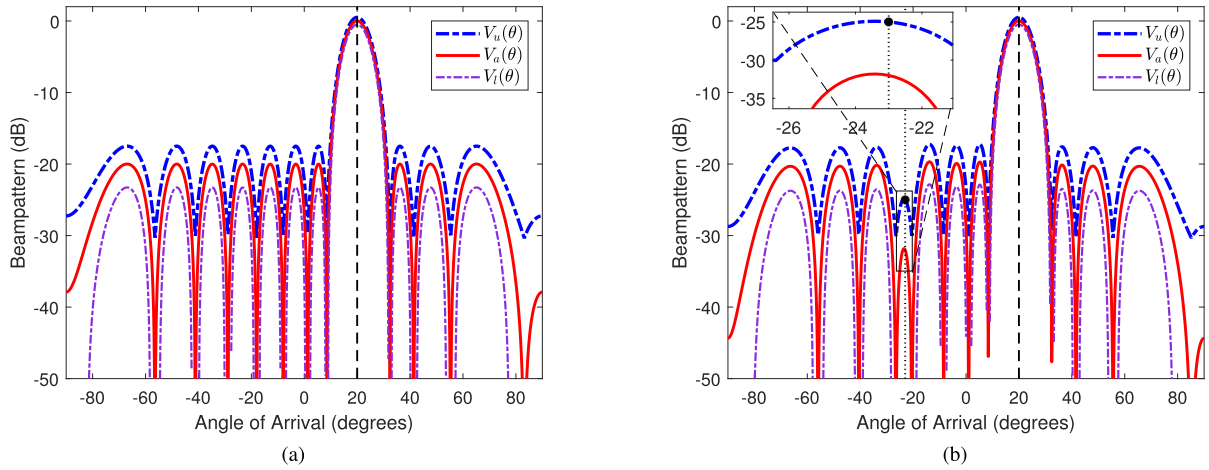

Fig. 3. Illustration of response control for a ULA. (a) Before array response control. (b) After array response control.

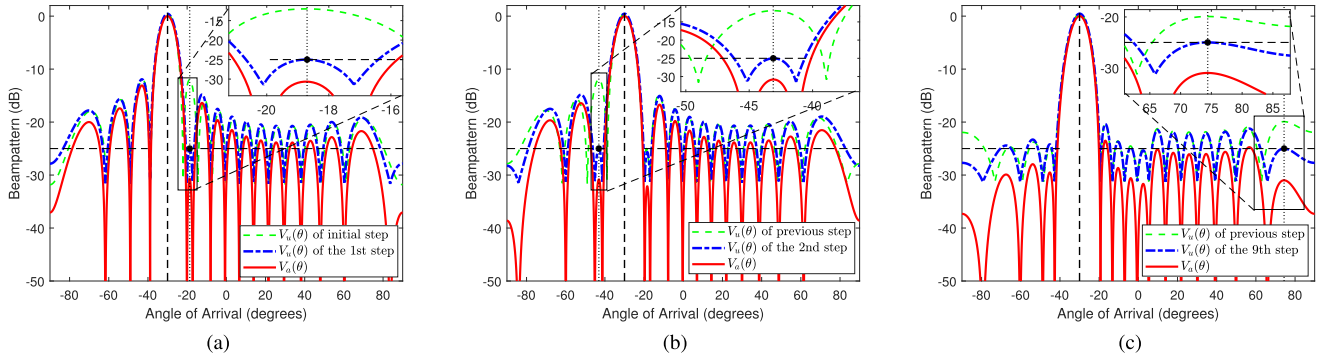

Fig. 4. Synthesis procedure of uniform-sidelobe pattern using a ULA. (a) Synthesized pattern at the first step. (b) Synthesized pattern at the second step. (c) Synthesized pattern at the ninth step.

beampattern $V_a(\theta)$ of the initial weight vector $\mathbf{w}_0 = \mathbf{a}(\theta_0)$, the corresponding worst-case upper boundary pattern $V_u(\theta)$ and the lower boundary pattern $V_l(\theta)$.

Applying our robust C^2-WORD algorithm and after some calculation, we can figure out that $\rho_{a,\star} = -42.7746$ dB, $\beta_{1,\star} = 0.077$. Fig. 2(b) presents the resulting beampatterns of the weight vector $\mathbf{w}_1$. It is shown that the upper boundary response level at θ_1 [i.e., $V_u(\theta_1)$] has been precisely adjusted to be $V_d(\theta_1) = -25$ dB. Since $V_u(\theta)$ is the worst-case upper boundary of the sidelobe response, we know that all the actual response level at θ_1 is lower than $V_u(\theta_1)$, if only $\|\Delta(\theta)\|_2 \leq \varepsilon(\theta)$ is satisfied. In addition, comparing to the beampatterns in Fig. 2(a), it should be noted that the resulting beampatterns in Fig. 2(b) are almost unchanged at the uncontrolled points (i.e., $\theta \neq \theta_1$).

To further show that our algorithm is effective for an arbitrarily specified initial weight, we consider a 12-element ULA and steer its beam axis to $\theta_0 = 20°$. In this case, we take the initial weight of robust C^2-WORD as the Chebyshev weight with a -20 dB sidelobe attenuation. The norm boundary of steering vector uncertainty is taken as $\varepsilon(\theta) = 0.1$. It is required to adjust the (actual) response level at $\theta_1 = -23°$ to be lower than $V_d(\theta_1) = -25$ dB. Fig. 3(a) shows the corresponding $V_a(\theta)$, $V_u(\theta)$ and $V_l(\theta)$ of the initial weight. After carrying out the proposed robust C^2-WORD scheme, we obtain that $\rho_{a,\star} = -31.9987$ dB and $\beta_{1,\star} = 0.2506$. The resulting beampatterns are presented in Fig. 3(b), from which we find that the value of $V_u(\theta_1)$ equals exactly to $V_d(\theta_1) = -25$ dB. Also, it can be checked from Fig. 3 that our algorithm results in small pattern variations at the unadjusted points after the robust sidelobe control process.

B. Robust Sidelobe Synthesis Using Robust C^2-WORD

In this section, representative simulations are presented to illustrate the application of robust C^2-WORD to sidelobe synthesis in the presence of steering vector uncertainties.

1) Uniform Sidelobe Synthesis for a ULA: In the first example, a 16-element ULA is considered. We steer the beam axis to $\theta_0 = -30°$. The desired upper beampattern has -25 dB uniform sidelobe level and the steering vector uncertainty $\Delta(\theta)$ is assumed to be norm-bounded by $\varepsilon(\theta) = 0.1$.

Fig. 4 presents several intermediate results when synthesizing pattern with robust C^2-WORD algorithm. In the first step, our algorithm compares the worst-case upper boundary pattern $V_{u,0}(\theta)$ of the initial weight with the desired pattern $V_d(\theta)$. Then, we choose $\theta_1 = -18.7°$ according to our angle selection strategy. Applying robust C^2-WORD, we figure out that $\rho_{a,\star} = -30.6544$ dB and $\beta_{1,\star} = 0.1276$ in the first step. The resulting beampatterns are depicted in Fig. 4(a), from which we can see that the upper boundary response level $V_{u,1}(\theta_1)$ has been precisely adjusted as its desired level (i.e., -25 dB). Based on

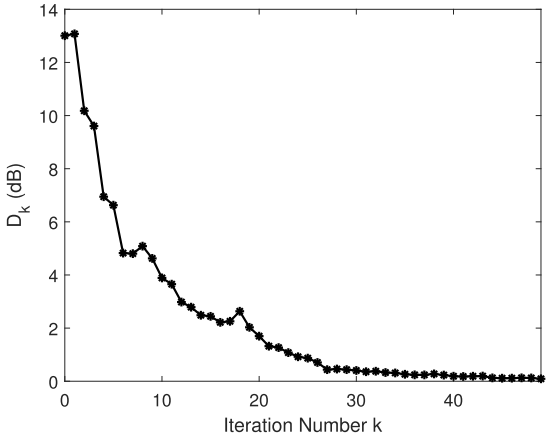

Fig. 5. Maximum response deviation D_k versus the iteration number.

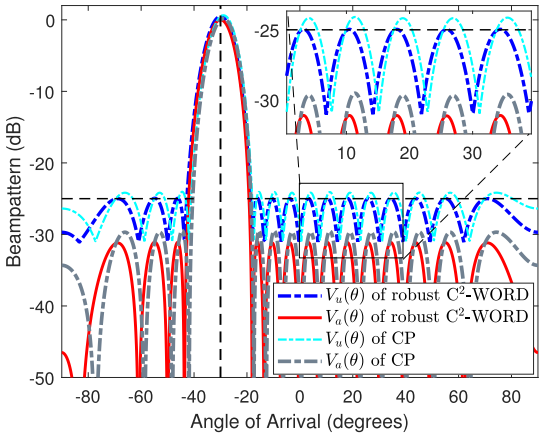

Fig. 6. Synthesized patterns with uniform sidelobe for a ULA.

TABLE II

OBTAINED WEIGHTINGS OF ROBUST C^2-WORD WHEN SYNTHESIZING UNIFORM SIDELOBE PATTERN FOR A ULA

n	w_n	n	w_n	n	w_n
1	$0.09e^{-j0.80}$	7	$0.34e^{+j2.35}$	13	$0.21e^{-j0.78}$
2	$0.11e^{-j2.37}$	8	$0.36e^{+j0.78}$	14	$0.16e^{-j2.35}$
3	$0.16e^{+j2.35}$	9	$0.36e^{-j0.78}$	15	$0.11e^{+j2.37}$
4	$0.21e^{+j0.78}$	10	$0.34e^{-j2.35}$	16	$0.09e^{+j0.80}$
5	$0.26e^{-j0.79}$	11	$0.31e^{+j2.36}$		
6	$0.31e^{-j2.36}$	12	$0.26e^{+j0.79}$		

TABLE III

OBTAINED WEIGHTINGS OF ROBUST C^2-WORD WITH CHANNEL PHASE-GAIN MISMATCH

n	w_n	n	w_n	n	w_n
1	$0.08e^{-j1.56}$	7	$0.36e^{+j3.10}$	13	$0.14e^{-j0.69}$
2	$0.10e^{+j1.42}$	8	$0.40e^{-j2.69}$	14	$0.13e^{-j2.21}$
3	$0.12e^{-j2.16}$	9	$0.39e^{-j2.71}$	15	$0.10e^{+j1.36}$
4	$0.14e^{-j0.60}$	10	$0.36e^{+j3.06}$	16	$0.08e^{-j1.67}$
5	$0.26e^{+j0.97}$	11	$0.31e^{+j2.26}$		
6	$0.31e^{+j2.31}$	12	$0.26e^{+j0.93}$		

the resulting $\mathbf{w}_1$ and $V_{u,1}(\theta)$, we conduct the second step of robust C^2-WORD algorithm and figure out that $\theta_2 = -43.1°$, $\rho_{a,\star} = -30.8132$ dB and $\beta_{1,\star} = 0.1245$. The obtained beampatterns are illustrated in Fig. 4(b), from which we can check that $V_{u,2}(\theta_2) = -25$ dB. Moreover, it can be observed that our algorithm results in small pattern variations at the uncontrolled region. After applying the robust C^2-WORD algorithm iteratively, the envelope of $V_u(\theta)$ becomes closer to $V_d(\theta)$, and we can terminate the iteration if a satisfactory $V_u(\theta)$ has been synthesized.

To explore the convergence of the proposed approach, we define D_k to measure the maximum response deviation within the set of sidelobe peak angles at the kth step (denoted by $\mathbf{\Omega}_s^k$)

$$D_k \triangleq \max_{\theta \in \mathbf{\Omega}_s^k} \left(V_{u,k}(\theta) - V_d(\theta) \right). \tag{63}$$

The curve of D_k versus the iterative number k is depicted in Fig. 5. It clearly shows that D_k decreases with the increase of iteration. After carrying out 50 response control steps, the resulting D_k approximately equals to zero and we terminate the synthesis process. Table II presents the resulting weight vector of our algorithm. Interestingly, it is found that the weights are centro-symmetric. A possible explanation is that the array utilized has a symmetrical structure.

The ultimate beampatterns are depicted in Fig. 6. We can see that the resulting worst-case upper boundary pattern $V_u(\theta)$ of our algorithm aligns with the desired upper sidelobe level. For the CP method in [8], we set the main lobe region as $[-42°, -18°]$ and obtain an upper boundary pattern $V_u(\theta)$ with a uniform sidelobe level, as shown in Fig. 6. For CP approach, the resulting maximum sidelobe level of $V_u(\theta)$ is about -24 dB, which is higher than that of the proposed robust C^2-WORD algorithm. In fact, there is a tradeoff between the main lobe width and the sidelobe level for CP method. Moreover, it is not clear how to determine the main lobe width of CP approach for a given sidelobe level requirement. In addition, the running time of the robust C^2-WORD algorithm is 0.03 s, which is much shorter than the 0.61 s of the CP method.

To further investigate the performance of the robust C^2-WORD algorithm with different discretization precisions, we measure the execution time T, and the resulting maximum sidelobe peak deviation (denoted as D_*) of the ultimate $V_u(\theta)$ away from the desired $V_d(\theta)$, by varying the angular discretization interval from 0.05° to 2.1°. Fig. 7 depicts the resulting curves of T and D_* versus the discretization interval. Generally speaking, less execution time T [see Fig. 7(a)] but worse performance [see D_* in Fig. 7(b)] are resulted, with the increase of the discretization interval. Moreover, even using a dense discretization (for example, discretizing the angular sector with interval 0.05°), the proposed robust C^2-WORD algorithm runs fast and can be completed within 0.1 s.

2) Uniform Sidelobe Synthesis With Channel Gain-Phase Mismatch: In this example, we consider a circular arc array with 16 nonisotropic elements, see Fig. 8 in [36] with $\theta_c = 60°$. The beam axis is taken as $\theta_0 = 0°$ and the sidelobe level is expected to be lower than -20 dB. The distance between adjacent elements is half a wavelength and there exist channel gain-phase uncertainties on sensor elements. More

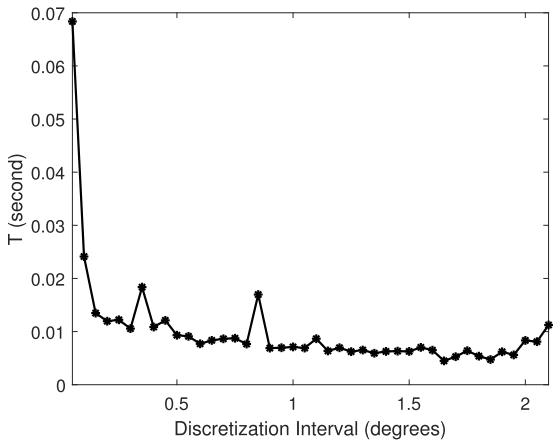

(a)

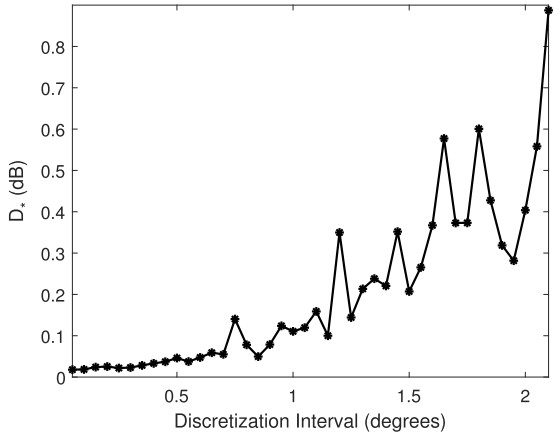

(b)

Fig. 7. Resulting curves with different discretization intervals. (a) Curve of the execution time T versus the discretization interval. (b) Curve of the maximum deviation D_* versus the discretization interval.

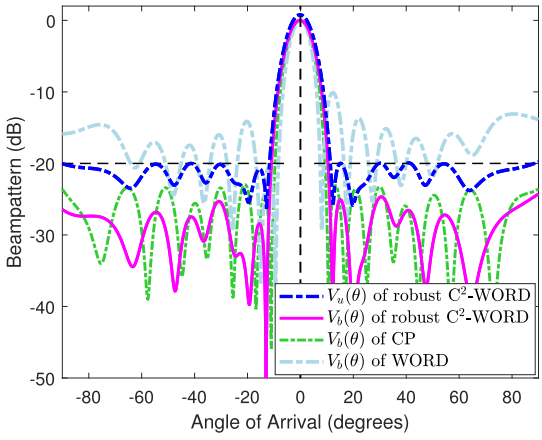

Fig. 8. Synthesized patterns for a circular arc array with gain-phase mismatch.

specifically, the phase error φ_n and gain error g_n are uniformly distributed in $[-0.035, 0.035]$ and $[0.98, 1.02]$, respectively, $n = 2, \ldots, N$. Following the analysis in Section III-A, we can figure out $\delta_1 = 0.039$ and then obtain the upper norm boundary $\varepsilon(\theta)$ according to (55).

Fig. 8 presents the resulting worst-case upper boundary pattern $V_u(\theta)$ of robust C^2-WORD algorithm after 20 iteration steps, and Table III lists the obtained weight vector. It can be clearly observed that the sidelobe envelope of $V_u(\theta)$ is aligned with the desired upper pattern $V_d(\theta)$. To compare the performances of different approaches, Fig. 8 also demonstrates the realizations of actual beampattern $V_b(\theta)$. We can see that the actual beampatterns of robust C^2-WORD and CP satisfy the preassigned response requirement, while the WORD algorithm does not. In this case, the execution time of the robust C^2-WORD algorithm is 0.06 s, and the counterpart of the CP method is 3.69 s.

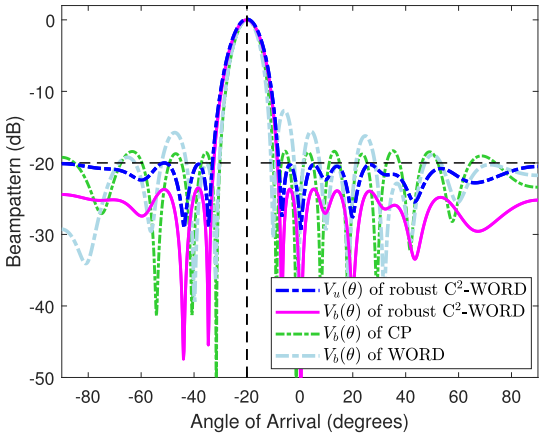

Fig. 9. Synthesized patterns for a linear array with element position mismatch.

3) Uniform Sidelobe Synthesis With Element Position Mismatch: We now carry out robust uniform sidelobe synthesis by considering array element position mismatch. More specifically, we use a 12-element nonuniformly spaced linear array, see Table I for its (ideal) element positions. The beam axis is steered to $\theta_0 = -20°$ and the upper level of the desired sidelobe response is -20 dB. The array suffers from element position perturbation and the location deviation is uniformly distributed in $[-0.5\%\lambda, 0.5\%\lambda]$. Under these settings, we can determine $\varepsilon(\theta)$ according to (58) and realize robust sidelobe synthesis using our robust C^2-WORD algorithm.

Fig. 9 presents the resulting $V_u(\theta)$ of robust C^2-WORD algorithm after 50 iteration steps, and Table IV gives the obtained weight vector. As expected, the obtained upper boundary beampattern $V_u(\theta)$ satisfies the preassigned response requirement. To show the superiority of our algorithm, we also depict the realizations of actual beampattern $V_b(\theta)$ for different methods. Fig. 9 shows that the actual beampatterns of CP and WORD result unqualified responses on sidelobe region. For the robust C^2-WORD algorithm, the obtained $V_b(\theta)$ meets our requirement with a sidelobe level about -25 dB. In addition, the running time of the robust C^2-WORD algorithm is 0.08 s, which is shorter than the 3.36 s of the CP method.

4) Nonuniform Sidelobe Synthesis With Mutual Coupling Effect: In this example, we consider a 20-element ULA and set the beam axis as $\theta_0 = -30°$. Following the mutual coupling model in Section III-C, we take mutual coupling effect into consideration by setting the channel coupling level as

TABLE IV

OBTAINED WEIGHTINGS OF ROBUST C^2-WORD WITH ELEMENT POSITION MISMATCH

n	w_n	n	w_n	n	w_n
1	$0.11e^{-j0.16}$	5	$0.37e^{+j1.78}$	9	$0.27e^{-j2.60}$
2	$0.23e^{-j0.89}$	6	$0.40e^{+j0.77}$	10	$0.22e^{+j2.73}$
3	$0.26e^{-j2.17}$	7	$0.37e^{-j0.40}$	11	$0.17e^{+j1.80}$
4	$0.36e^{+j2.90}$	8	$0.37e^{-j1.47}$	12	$0.12e^{+j0.62}$

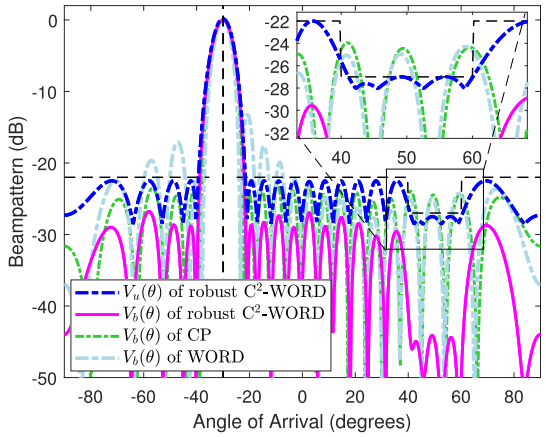

Fig. 10. Synthesized patterns for a ULA with mutual coupling effect.

TABLE V

OBTAINED WEIGHTINGS OF ROBUST C^2-WORD WITH MUTUAL COUPLING EFFECT

n	w_n	n	w_n	n	w_n
1	$0.10e^{-j0.07}$	8	$0.28e^{+j1.58}$	15	$0.23e^{+j3.14}$
2	$0.11e^{-j1.37}$	9	$0.31e^{+j0.01}$	16	$0.20e^{+j1.55}$
3	$0.13e^{+j3.01}$	10	$0.31e^{-j1.59}$	17	$0.15e^{-j0.06}$
4	$0.15e^{+j1.64}$	11	$0.31e^{-j3.12}$	18	$0.13e^{-j1.44}$
5	$0.20e^{+j0.02}$	12	$0.31e^{+j1.56}$	19	$0.11e^{+j2.94}$
6	$0.23e^{-j1.57}$	13	$0.28e^{-j0.01}$	20	$0.10e^{+j1.65}$
7	$0.26e^{-j3.14}$	14	$0.26e^{-j1.57}$		

$\xi = -35$ dB. With these configurations, one can readily determine the upper boundary $\varepsilon(\theta)$ according to (62). Different from the previous testings, in this case, we consider a nonuniform desired upper sidelobe in $V_d(\theta)$. More specifically, the upper level is -27 dB in the region $[40°, 60°]$ and -22 dB in the rest of the sidelobe region.

Fig. 10 shows the resulting $V_u(\theta)$ of the proposed robust C^2-WORD algorithm after 80 iteration steps, and Table V lists the corresponding weight vector. Though the desired sidelobe level is nonuniform, we can see clearly that $V_u(\theta)$ satisfies the preassigned requirement. Fig. 10 also depicts the realizations of actual beampattern [i.e., $V_b(\theta)$] for robust C^2-WORD, CP and WORD. It is observed that the robust C^2-WORD algorithm obtains a qualified beampattern $V_b(\theta)$ with nonuniform sidelobe shape. The resulting sidelobe of CP method is uniform and does not satisfy the preassigned requirement in the null region. As for WORD, the maximal sidelobe level of $V_b(\theta)$ is about -13 dB, which is also an undesirable result. In addition, the running time of the CP method is 3.41 s, which is longer than the 0.08 s of the proposed robust C^2-WORD algorithm.

VI. CONCLUSION

In this paper, we have presented a new scheme named complex-coefficient weight vector orthogonal decomposition (C^2-WORD). The C^2-WORD algorithm is modified from the existing WORD method, and is able to precisely control the array response level of a given point starting from an arbitrarily specified weight vector. Based on C^2-WORD, we have devised a robust C^2-WORD algorithm, which can realize robust sidelobe control and synthesis in the presence of steering vector mismatch. Assuming that the steering vector uncertainty is norm-bounded, the robust C^2-WORD algorithm precisely adjusts the worst-case upper boundary response of a given sidelobe point as the desired level. The proposed robust C^2-WORD algorithm has an analytical expression of weight vector updating and runs faster than the conventional convex programming method. We have also presented detailed analyses on how to determine the norm boundary of steering vector uncertainty under various mismatch circumstances. Moreover, a robust sidelobe synthesis approach has been devised by successively applying robust C^2-WORD algorithm. The applications of robust C^2-WORD to robust sidelobe control and synthesis have been validated with various examples. As a future work, we shall consider the robust multi-point response control algorithm so as to reduce the number of iterations steps in pattern synthesis process.

APPENDIX A
DERIVATION OF (11)

Substituting (10b) into (10a) and recalling the constraint $L_k(\theta_k, \theta_0) = \rho_k$, we have

$$G(\mathbf{w}_k) \propto J(\beta_k) \triangleq \frac{|\beta_k|^2 \left|\mathbf{w}_\parallel^{\mathrm{H}} \mathbf{a}(\theta_k)\right|^2}{\|\mathbf{w}_\perp\|_2^2 + |\beta_k|^2 \|\mathbf{w}_\parallel\|_2^2}. \tag{64}$$

On this basis, it is not hard to derive that

$$\frac{\partial J(\beta_k)}{\partial |\beta_k|^2} = \frac{\left|\mathbf{w}_\parallel^{\mathrm{H}} \mathbf{a}(\theta_k)\right|^2 \|\mathbf{w}_\perp\|_2^2}{\left(\|\mathbf{w}_\perp\|_2^2 + |\beta|^2 \|\mathbf{w}_\parallel\|_2^2\right)^2} \geq 0 \tag{65}$$

which implies that $J(\beta_k)$ is monotonically nondecreasing with the increase of $|\beta_k|$. According to this observation, one can readily obtain that

$$\beta_{k,\triangleright} = \arg \max_{\beta_k \in \mathbb{C}_{\beta_k}} |\beta_k|. \tag{66}$$

Recalling Fig. 1, we know that the β_k with maximum modulo among $\mathbb{C}_{\beta_k}$ is the intersection point of circle $\mathbb{C}_{\beta_k}$ with the line that passes O and $\mathbf{c}_{\beta_k}$ [see $g^{-1}(\beta_{k,l})$ in Fig. 1]. Mathematically, it can be readily obtained that

$$\beta_{k,\triangleright} = (|\mathbf{c}_{\beta_k}| + R_{\beta_k}) e^{j \angle g(\mathbf{c}_{\beta_k})}. \tag{67}$$

This completes the derivation of (11).

$$\left(\frac{\rho_a\left|\mathbf{w}_\perp^{\mathrm{H}}\mathbf{a}(\theta_0)\right|\cdot\left|\mathbf{w}_\parallel^{\mathrm{H}}\mathbf{a}(\theta_0)\right|+\sqrt{\rho_a}\left|\mathbf{w}_\perp^{\mathrm{H}}\mathbf{a}(\theta_0)\right|\cdot\left|\mathbf{w}_\parallel^{\mathrm{H}}\mathbf{a}(\theta_k)\right|}{\left|\left|\mathbf{w}_\parallel^{\mathrm{H}}\mathbf{a}(\theta_k)\right|^2-\rho_a\left|\mathbf{w}_\parallel^{\mathrm{H}}\mathbf{a}(\theta_0)\right|^2\right|}\right)^2=\frac{\left(\frac{\sqrt{\rho_a}\gamma\,(\theta_k)}{V_d(\theta_k)-\sqrt{\rho_a}}\right)^2\|\mathbf{w}_\perp\|_2^2}{\left|\mathbf{w}_\parallel^{\mathrm{H}}\mathbf{a}(\theta_k)\right|^2-\left(\frac{\sqrt{\rho_a}\gamma\,(\theta_k)}{V_d(\theta_k)-\sqrt{\rho_a}}\right)^2\|\mathbf{w}_\parallel\|_2^2} \tag{77}$$

$$A=\left(\left|\mathbf{w}_\parallel^{\mathrm{H}}\mathbf{a}(\theta_k)\right|^2-\gamma^2(\theta_k)\|\mathbf{w}_\parallel\|_2^2\right)\cdot\left|\mathbf{w}_\perp^{\mathrm{H}}\mathbf{a}(\theta_0)\right|^2\cdot\left|\mathbf{w}_\parallel^{\mathrm{H}}\mathbf{a}(\theta_0)\right|^2-\gamma^2(\theta_k)\|\mathbf{w}_\perp\|_2^2\cdot\left|\mathbf{w}_\parallel^{\mathrm{H}}\mathbf{a}(\theta_0)\right|^4 \tag{79a}$$

$$B=2\left(\left(\left|\mathbf{w}_\parallel^{\mathrm{H}}\mathbf{a}(\theta_k)\right|^2-\gamma^2(\theta_k)\|\mathbf{w}_\parallel\|_2^2\right)-V_d(\theta_k)\cdot\left|\mathbf{w}_\parallel^{\mathrm{H}}\mathbf{a}(\theta_0)\right|\left|\mathbf{w}_\parallel^{\mathrm{H}}\mathbf{a}(\theta_k)\right|\right)\left|\mathbf{w}_\perp^{\mathrm{H}}\mathbf{a}(\theta_0)\right|^2\cdot\left|\mathbf{w}_\parallel^{\mathrm{H}}\mathbf{a}(\theta_0)\right|\cdot\left|\mathbf{w}_\parallel^{\mathrm{H}}\mathbf{a}(\theta_k)\right| \tag{79b}$$

$$\begin{aligned}C=\;&V_d^2(\theta_k)\left|\mathbf{w}_\parallel^{\mathrm{H}}\mathbf{a}(\theta_k)\right|^2\cdot\left|\mathbf{w}_\perp^{\mathrm{H}}\mathbf{a}(\theta_0)\right|^2\cdot\left|\mathbf{w}_\parallel^{\mathrm{H}}\mathbf{a}(\theta_0)\right|^2+\left(\left|\mathbf{w}_\parallel^{\mathrm{H}}\mathbf{a}(\theta_k)\right|^2-\gamma^2(\theta_k)\|\mathbf{w}_\parallel\|_2^2\right)\cdot\left|\mathbf{w}_\parallel^{\mathrm{H}}\mathbf{a}(\theta_k)\right|^2\cdot\left|\mathbf{w}_\perp^{\mathrm{H}}\mathbf{a}(\theta_0)\right|^2\\&-4V_d(\theta_k)\left|\mathbf{w}_\parallel^{\mathrm{H}}\mathbf{a}(\theta_k)\right|^3\cdot\left|\mathbf{w}_\parallel^{\mathrm{H}}\mathbf{a}(\theta_0)\right|\cdot\left|\mathbf{w}_\perp^{\mathrm{H}}\mathbf{a}(\theta_0)\right|^2+2\gamma^2(\theta_k)\|\mathbf{w}_\perp\|_2^2\cdot\left|\mathbf{w}_\parallel^{\mathrm{H}}\mathbf{a}(\theta_k)\right|^2\cdot\left|\mathbf{w}_\parallel^{\mathrm{H}}\mathbf{a}(\theta_0)\right|^2\end{aligned} \tag{79c}$$

$$D=2V_d(\theta_k)\left|\mathbf{w}_\parallel^{\mathrm{H}}\mathbf{a}(\theta_k)\right|^3\cdot\left|\mathbf{w}_\perp^{\mathrm{H}}\mathbf{a}(\theta_0)\right|^2\cdot\left(V_d(\theta_k)\left|\mathbf{w}_\parallel^{\mathrm{H}}\mathbf{a}(\theta_0)\right|-\left|\mathbf{w}_\parallel^{\mathrm{H}}\mathbf{a}(\theta_k)\right|\right) \tag{79d}$$

$$E=\left|\mathbf{w}_\parallel^{\mathrm{H}}\mathbf{a}(\theta_k)\right|^4\cdot\left(V_d^2(\theta_k)\left|\mathbf{w}_\perp^{\mathrm{H}}\mathbf{a}(\theta_0)\right|^2-\gamma^2(\theta_k)\cdot\|\mathbf{w}_\perp\|_2^2\right) \tag{79e}$$

APPENDIX B
DERIVATION OF (33)

To simplify the notation, we omit the subscript of β in sequel. According to the definition of ρ_a in (32), we have

$$\sqrt{\rho_a}=\left|\mathbf{w}_k^{\mathrm{H}}\mathbf{a}(\theta_k)\right|/\left|\mathbf{w}_k^{\mathrm{H}}\mathbf{a}(\theta_0)\right|. \tag{68}$$

Recalling the constraint (30b), we can expand it as

$$\begin{aligned}\sqrt{\rho_a}&=V_d(\theta_k)-\frac{\gamma\,(\theta_k)\|\mathbf{w}_k\|_2}{\left|\mathbf{w}_k^{\mathrm{H}}\mathbf{a}(\theta_0)\right|}\\&=V_d(\theta_k)-\frac{\sqrt{\rho_a}\gamma\,(\theta_k)\|\mathbf{w}_k\|_2}{\left|\mathbf{w}_k^{\mathrm{H}}\mathbf{a}(\theta_k)\right|}\end{aligned} \tag{69}$$

where (68) has been utilized. Substituting the constraint (30c) into $\mathbf{w}_k$, we obtain

$$\frac{\left|\mathbf{w}_k^{\mathrm{H}}\mathbf{a}(\theta_k)\right|^2}{\|\mathbf{w}_k\|_2^2}=\frac{|\beta|^2\left|\mathbf{w}_\parallel^{\mathrm{H}}\mathbf{a}(\theta_k)\right|^2}{\|\mathbf{w}_\perp\|_2^2+|\beta|^2\|\mathbf{w}_\parallel\|_2^2}. \tag{70}$$

Then, we can reformulate (69) as

$$V_d(\theta_k)-\sqrt{\rho_a}=\frac{\sqrt{\rho_a}\gamma\,(\theta_k)}{\sqrt{\dfrac{|\beta|^2\left|\mathbf{w}_\parallel^{\mathrm{H}}\mathbf{a}(\theta_k)\right|^2}{\|\mathbf{w}_\perp\|_2^2+|\beta|^2\|\mathbf{w}_\parallel\|_2^2}}} \tag{71}$$

or equivalently

$$|\beta|^2=\frac{\left(\frac{\sqrt{\rho_a}\gamma\,(\theta_k)}{V_d(\theta_k)-\sqrt{\rho_a}}\right)^2\|\mathbf{w}_\perp\|_2^2}{\left|\mathbf{w}_\parallel^{\mathrm{H}}\mathbf{a}(\theta_k)\right|^2-\left(\frac{\sqrt{\rho_a}\gamma\,(\theta_k)}{V_d(\theta_k)-\sqrt{\rho_a}}\right)^2\|\mathbf{w}_\parallel\|_2^2}. \tag{72}$$

On the other hand, we can see from (7) that

$$|\beta|=|\mathbf{c}_\beta|+R_\beta \tag{73}$$

with

$$|\mathbf{c}_\beta|=\frac{\rho_a\left|\mathbf{w}_\perp^{\mathrm{H}}\mathbf{a}(\theta_0)\right|\cdot\left|\mathbf{w}_\parallel^{\mathrm{H}}\mathbf{a}(\theta_0)\right|}{|\mathbf{B}(2,2)|} \tag{74}$$

$$R_\beta=\frac{\sqrt{\rho_a}\left|\mathbf{w}_\perp^{\mathrm{H}}\mathbf{a}(\theta_0)\right|\cdot\left|\mathbf{w}_\parallel^{\mathrm{H}}\mathbf{a}(\theta_k)\right|}{|\mathbf{B}(2,2)|} \tag{75}$$

where $\mathbf{B}$ is given by

$$\mathbf{B}=\begin{bmatrix}\mathbf{w}_\perp^{\mathrm{H}}\mathbf{a}(\theta_k)\\ \mathbf{w}_\parallel^{\mathrm{H}}\mathbf{a}(\theta_k)\end{bmatrix}\begin{bmatrix}\mathbf{w}_\perp^{\mathrm{H}}\mathbf{a}(\theta_k)\\ \mathbf{w}_\parallel^{\mathrm{H}}\mathbf{a}(\theta_k)\end{bmatrix}^{\mathrm{H}}-\rho_a\begin{bmatrix}\mathbf{w}_\perp^{\mathrm{H}}\mathbf{a}(\theta_0)\\ \mathbf{w}_\parallel^{\mathrm{H}}\mathbf{a}(\theta_0)\end{bmatrix}\begin{bmatrix}\mathbf{w}_\perp^{\mathrm{H}}\mathbf{a}(\theta_0)\\ \mathbf{w}_\parallel^{\mathrm{H}}\mathbf{a}(\theta_0)\end{bmatrix}^{\mathrm{H}}. \tag{76}$$

Thus, we have

$$|\beta|=\frac{\rho_a\left|\mathbf{w}_\perp^{\mathrm{H}}\mathbf{a}(\theta_0)\right|\cdot\left|\mathbf{w}_\parallel^{\mathrm{H}}\mathbf{a}(\theta_0)\right|+\sqrt{\rho_a}\left|\mathbf{w}_\perp^{\mathrm{H}}\mathbf{a}(\theta_0)\right|\cdot\left|\mathbf{w}_\parallel^{\mathrm{H}}\mathbf{a}(\theta_k)\right|}{\left|\left|\mathbf{w}_\parallel^{\mathrm{H}}\mathbf{a}(\theta_k)\right|^2-\rho_a\left|\mathbf{w}_\parallel^{\mathrm{H}}\mathbf{a}(\theta_0)\right|^2\right|}.$$

Substituting the above $|\beta|$ into (72), we can eliminate β and obtain a quartic equation with respect to ρ_a, as shown in (77) on the top of this page. After some manipulations, we can reshape (77) as

$$A\rho_a^2+B\rho_a\sqrt{\rho_a}+C\rho_a+D\sqrt{\rho_a}+E=0 \tag{78}$$

where the coefficients A, B, C, D and E are given in (79) on the top of this page. Equation (78) can be alternatively expressed as

$$A\rho_a^2+C\rho_a+E=-\sqrt{\rho_a}(B\rho_a+D). \tag{80}$$

Taking square to both sides of (80) yields

$$\begin{aligned}A^2\rho_a^4+(2AC-B^2)\rho_a^3+(2AE-2BD+C^2)\rho_a^2\\+(2CE-D^2)\rho_a+E^2=0.\end{aligned} \tag{81}$$

This completes the derivation of (33).

APPENDIX C
DERIVATIONS OF THE FEASIBILITY OF (33)

To study the feasibility of (33), it is reasonable to assume that $V_d(\theta_k)>0$. On this basis, we can substitute ρ_a in (32) and the constraint in (30c) into (30b), and obtain

$$\sqrt{\rho_a}=V_d(\theta_k)-\frac{\gamma\,(\theta_k)\|\mathbf{w}_k\|_2}{\left|\mathbf{w}_k^{\mathrm{H}}\mathbf{a}(\theta_0)\right|}. \tag{82}$$

Define

$$f(\rho_a)\triangleq V_d(\theta_k)-\sqrt{\rho_a}-\frac{\gamma\,(\theta_k)\|\mathbf{w}_k\|_2}{\left|\mathbf{w}_k^{\mathrm{H}}\mathbf{a}(\theta_0)\right|}. \tag{83}$$

Note that $\beta_\star = 0$ and $\mathbf{w}_k = \mathbf{w}_\perp$ when $\rho_a = 0$ applies. Then, we combine (44) and obtain that

$$\begin{aligned} f(0) &= V_d(\theta_k) - \frac{\gamma(\theta_k)\|\mathbf{w}_k\|_2}{\left|\mathbf{w}_k^{\mathrm{H}}\mathbf{a}(\theta_0)\right|} \\ &= V_d(\theta_k) - \frac{[V_d(\theta_k)\varepsilon(\theta_0) + \varepsilon(\theta_k)] \cdot \|\mathbf{w}_\perp\|_2}{\left|\mathbf{w}_\perp^{\mathrm{H}}\mathbf{a}(\theta_0)\right|} \\ &= V_d(\theta_k) \cdot \frac{\left(\left|\mathbf{w}_\perp^{\mathrm{H}}\mathbf{a}(\theta_0)\right| - \varepsilon(\theta_0)\|\mathbf{w}_\perp\|_2\right)}{\left|\mathbf{w}_\perp^{\mathrm{H}}\mathbf{a}(\theta_0)\right|} - \frac{\varepsilon(\theta_k)\|\mathbf{w}_\perp\|_2}{\left|\mathbf{w}_\perp^{\mathrm{H}}\mathbf{a}(\theta_0)\right|} \\ &\geq 0. \end{aligned} \tag{84}$$

On the other hand, we can readily check that

$$f(V_d^2(\theta_k)) = -\frac{\gamma(\theta_k)\|\mathbf{w}_k\|_2}{\left|\mathbf{w}_k^{\mathrm{H}}\mathbf{a}(\theta_0)\right|} < 0. \tag{85}$$

Since $f(\rho_a)$ in (83) is a continuous function, the results (84) and (85) indicate that there exists a $\breve{\rho}_a \in [0, V_d^2(\theta_k))$ such that

$$f(\breve{\rho}_a) = 0. \tag{86}$$

Recalling the derivations in appendix B, the quartic polynomial in (33) is derived from $f(\rho_a) = 0$. As a result, we learn from (86) that there exists the same $\breve{\rho}_a \in [0, V_d^2(\theta_k))$ solving the quartic polynomial (33). This completes the derivations.

ACKNOWLEDGMENT

The authors would like to thank the Editor and the anonymous reviewers for their valuable comments and suggestions.

REFERENCES

[1] M. H. Er, "Array pattern synthesis with a controlled mean-square sidelobe level," *IEEE Trans. Signal Process.*, vol. 40, no. 4, pp. 977–981, Apr. 1992.

[2] B. Fuchs and S. Rondineau, "Array pattern synthesis with excitation control via norm minimization," *IEEE Trans. Antennas Propag.*, vol. 64, no. 10, pp. 4228–4234, Oct. 2016.

[3] B. Fuchs and J. J. Fuchs, "Optimal narrow beam low sidelobe synthesis for arbitrary arrays," *IEEE Trans. Antennas Propag.*, vol. 58, no. 5, pp. 2130–2135, Jun. 2010.

[4] G. Oliveri, M. Salucci, and A. Massa, "Synthesis of modular contiguously clustered linear arrays through a sparseness-regularized solver," *IEEE Trans. Antennas Propag.*, vol. 64, no. 10, pp. 4277–4287, Oct. 2016.

[5] C.-C. Tseng and L. J. Griffiths, "A simple algorithm to achieve desired patterns for arbitrary arrays," *IEEE Trans. Signal Process.*, vol. 40, no. 11, pp. 2737–2746, Nov. 1992.

[6] X. Zhang, Z. He, B. Liao, X. Zhang, Z. Cheng, and Y. Lu, "A^{2}RC: An accurate array response control algorithm for pattern synthesis," *IEEE Trans. Signal Process.*, vol. 65, no. 7, pp. 1810–1824, Apr. 2017.

[7] X. Zhang, Z. He, X. Zhang, and W. Peng, "High-performance beampattern synthesis via linear fractional semidefinite relaxation and quasi-convex optimization," *IEEE Trans. Antennas Propag.*, vol. 66, no. 7, pp. 3421–3431, Jul. 2018.

[8] S. Yan and J. M. Hovem, "Array pattern synthesis with robustness against manifold vectors uncertainty," *IEEE J. Ocean. Eng.*, vol. 33, no. 4, pp. 405–413, Oct. 2008.

[9] T. Zhang and W. Ser, "Robust beampattern synthesis for antenna arrays with mutual coupling effect," *IEEE Trans. Antennas Propag.*, vol. 59, no. 8, pp. 2889–2895, Aug. 2011.

[10] M. S. Hossain, G. N. Milford, M. C. Reed, and L. C. Godara, "Robust efficient broadband antenna array pattern synthesis techniques," *IEEE Trans. Antennas Propag.*, vol. 62, no. 9, pp. 4537–4546, Sep. 2014.

[11] S. A. Vorobyov, A. B. Gershman, and Z.-Q. Luo, "Robust adaptive beamforming using worst-case performance optimization: A solution to the signal mismatch problem," *IEEE Trans. Signal Process.*, vol. 51, no. 2, pp. 313–324, Feb. 2003.

[12] B. Liao, K. M. Tsui, and S. C. Chan, "Robust beamforming with magnitude response constraints using iterative second-order cone programming," *IEEE Trans. Antennas Propag.*, vol. 59, no. 9, pp. 3477–3482, Sep. 2011.

[13] S. E. Nai, W. Ser, Z. L. Yu, and S. Rahardja, "A robust adaptive beamforming framework with beampattern shaping constraints," *IEEE Trans. Antennas Propag.*, vol. 57, no. 7, pp. 2198–2203, Jul. 2009.

[14] Z. L. Yu, M. H. Er, and W. Ser, "A novel adaptive beamformer based on semidefinite programming (SDP) with magnitude response constraints," *IEEE Trans. Antennas Propag.*, vol. 56, no. 5, pp. 1297–1307, May 2008.

[15] D. D. Feldman and L. J. Griffiths, "A projection approach for robust adaptive beamforming," *IEEE Trans. Signal Process.*, vol. 42, no. 4, pp. 867–876, Apr. 1994.

[16] L. Tenuti, N. Anselmi, P. Rocca, M. Salucci, and A. Massa, "Minkowski sum method for planar arrays sensitivity analysis with uncertain-but-bounded excitation tolerances," *IEEE Trans. Antennas Propag.*, vol. 65, no. 1, pp. 167–177, Jan. 2017.

[17] N. Anselmi, L. Manica, P. Rocca, and A. Massa, "Tolerance analysis of antenna arrays through interval arithmetic," *IEEE Trans. Antennas Propag.*, vol. 61, no. 11, pp. 5496–5507, Nov. 2013.

[18] P. Rocca, N. Anselmi, and A. Massa, "Optimal synthesis of robust beamformer weights exploiting interval analysis and convex optimization," *IEEE Trans. Antennas Propag.*, vol. 62, no. 7, pp. 3603–3612, Jul. 2014.

[19] L. Poli, P. Rocca, N. Anselmi, and A. Massa, "Dealing with uncertainties on phase weighting of linear antenna arrays by means of interval-based tolerance analysis," *IEEE Trans. Antennas Propag.*, vol. 63, no. 7, pp. 3229–3234, Jul. 2015.

[20] N. Hu, B. Duan, W. Xu, and J. Zhou, "A new interval pattern analysis method of array antennas based on Taylor expansion," *IEEE Trans. Antennas Propag.*, vol. 65, no. 11, pp. 6151–6156, Nov. 2017.

[21] X. Zhang, Z. He, B. Liao, X. Zhang, and W. Peng, "Pattern synthesis for arbitrary arrays via weight vector orthogonal decomposition," *IEEE Trans. Signal Process.*, vol. 66, no. 5, pp. 1286–1299, Mar. 2018.

[22] R. C. Nongpiur and D. J. Shpak, "Synthesis of linear and planar arrays with minimum element selection," *IEEE Trans. Signal Process.*, vol. 62, no. 20, pp. 5398–5410, Oct. 2014.

[23] H. Cox, R. Zeskind, and M. Owen, "Robust adaptive beamforming," *IEEE Trans. Acoust., Speech, Signal Process.*, vol. ASSP-35, no. 10, pp. 1365–1376, Oct. 1987.

[24] H. Cox, R. Zeskind, and T. Kooij, "Practical supergain," *IEEE Trans. Acoust., Speech, Signal Process.*, vol. ASSP-34, no. 3, pp. 393–398, Jun. 1986.

[25] S. L. Shmakov, "A Universal method of solving quartic equations," *Int. J. Pure Appl. Math.*, vol. 71, no. 2, pp. 251–259, 2011.

[26] G. H. Golub and C. F. V. Loan, *Matrix Computations*. Baltimore, MD, USA: Baltimore, MD, USA: The Johns Hopkins Univ. Press, 1996.

[27] C. M. Schmid, S. Schuster, R. Feger, and A. Stelzer, "On the effects of calibration errors and mutual coupling on the beam pattern of an antenna array," *IEEE Trans. Antennas Propag.*, vol. 61, no. 8, pp. 4063–4072, Aug. 2013.

[28] B. Liao and S. C. Chan, "Direction finding with partly calibrated uniform linear arrays," *IEEE Trans. Antennas Propag.*, vol. 60, no. 2, pp. 922–929, Feb. 2012.

[29] N. Boon Chong and C. M. S. See, "Sensor-array calibration using a maximum-likelihood approach," *IEEE Trans. Antennas Propag.*, vol. 44, no. 6, pp. 827–835, Jun. 1996.

[30] M. Zhang and Z. Zhu, "A method for direction finding under sensor gain and phase uncertainties," *IEEE Trans. Antennas Propag.*, vol. 43, no. 8, pp. 880–883, Aug. 1995.

[31] K. C. Ho and L. Yang, "On the use of a calibration emitter for source localization in the presence of sensor position uncertainty," *IEEE Trans. Signal Process.*, vol. 56, no. 12, pp. 5758–5772, Dec. 2008.

[32] B. Friedlander and A. Weiss, "Direction finding in the presence of mutual coupling," *IEEE Trans. Antennas Propag.*, vol. 39, no. 3, pp. 273–284, Mar. 1991.

[33] D. F. Kelley and W. L. Stutzman, "Array antenna pattern modeling methods that include mutual coupling effects," *IEEE Trans. Antennas Propag.*, vol. 41, no. 12, pp. 1625–1632, Dec. 1993.

[34] Q. Yuan, Q. Chen, and K. Sawaya, "Performance of adaptive array antenna with arbitrary geometry in the presence of mutual coupling," *IEEE Trans. Antennas Propag.*, vol. 54, no. 7, pp. 1991–1996, Jul. 2006.

[35] J. W. Demmel, *Applied Numerical Linear Algebra*. Philadelphia, PA, USA: SIAM, 1997.

[36] X. Zhang, Z. He, B. Liao, X. Zhang, and W. Peng, "Pattern synthesis with multipoint accurate array response control," *IEEE Trans. Antennas Propag.*, vol. 65, no. 8, pp. 4075–4088, Aug. 2017.

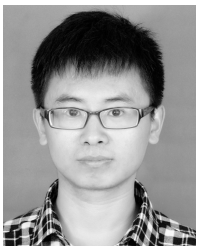

Xuejing Zhang (S'17) was born in Hebei, China. He received the B.S. degree in electrical engineering from Huaqiao University, Xiamen, China, and the M.S. degree in signal and information processing from Xidian University, Xi'an, China, in 2011 and 2014, respectively. He is currently pursuing the Ph.D. degree in signal and information processing with the School of Information and Communication Engineering, University of Electronic Science and Technology of China (UESTC), Chengdu, China.

Since 2017, he has been a Visiting Student with the University of Delaware, Newark, DE, USA. His current research interests include array signal processing and wireless communications.

Zishu He (M'11) was born in Sichuan, China, in 1962. He received the B.S., M.S., and Ph.D. degrees in signal and information processing from the University of Electronic Science and Technology of China (UESTC), Chengdu, China, in 1984, 1988, and 2000, respectively.

He is currently a Professor with the School of Information and Communication Engineering, UESTC. His current research interests include array signal processing, digital beam forming, the theory on multiple-input multiple-output (MIMO) communication, and MIMO radar, adaptive signal processing and interference cancellation.

Xuepan Zhang was born in Hebei, China. He received the B.S. degree in electrical engineering from Xidian University, Xi'an, China, in 2010, and the Ph.D. degree from the National Laboratory of Radar Signal Processing, Xidian University, in 2015, respectively.

He is currently a Principal Investigator with the Qian Xuesen Laboratory of Space Technology, Beijing, China. His current research interests include synthetic aperture radar (SAR), ground moving target indication (GMTI), and deep learning.

Julan Xie was born in Leiyang, China. She received the B.S. and Ph.D. degrees in signal and information processing from the University of Electronic Science and Technology of China (UESTC), Chengdu, China, in 2005 and 2012, respectively.

She is currently an Associate Professor of signal and information processing with the School of Information and Communication Engineering, UESTC. Her current research interests include array signal processing, digital beam forming, interference cancellation, and array optimization.